Timing and mechanisms of Tibetan Plateau uplift

Lin Ding^{1†}, Paul Kapp², Fulong Cai^{1†}, Carmala N. Garzione², Zhongyu Xiong¹, Houqi Wang¹ and Chao Wang¹

- State Key Laboratory of Tibetan Plateau Earth System Science, Resources and Environment, Institute of Tibetan Plateau Research, Chinese Academy of Sciences, Beijing, China
- ² Department of Geosciences, University of Arizona, Tucson, Arizona, U.S.A.

Key points

- The Tibetan Plateau did not get uplifted as a large entity or grow systematically outward from the India—Asia suture (IAS), because lithospheric heterogeneities in Asia imparted by pre-Cenozoic tectonic events created relatively weak and strong zones that deformed differently during collision.
- Cretaceous tectonic events built embryonic mountains belts and weakened the lithosphere in southern and central Tibet.
- Continental Asian detritus appeared in Indian continental margin sedimentary rocks by 65–60 million years ago (Ma). The most conservative interpretation based on available geologic constraints is that these sediments mark the initiation of India–Asia collision.
- The quest to further quantify the history of surface elevation change across Tibet spurred the field of quantitative palaeo-altimetry, such as measurement of oxygen and hydrogen isotopes in palaeo-water proxies, carbonate clumped isotope thermometry and fossil leaf physiognomy.
- Quantitative palaeo-altimetry suggests that high (≥4 km) elevations were obtained in southern Tibet by ~55 Ma and in central Tibet by ~45 Ma, whereas an intervening valley remained at <2 km elevation until between ~38 and 29 Ma. The IAS zone and Himalaya Mountains were rapidly uplifted from <3 km to near-modern elevations at ~20 Ma.</p>
- Subcrustal processes such as subduction, delamination and break-off of Indian and Asian continental lithosphere were important tectonic events during the formation of the Tibetan Plateau.

Abstract

The timing of the initial India-Asia collision and the mechanisms that led to the eventual formation of the high (>5 km) Tibetan Plateau remain enigmatic. In this Review, we describe the spatio-temporal distribution and geodynamic mechanisms of surface uplift in the Tibetan Plateau, based on geologic and palaeo-altimetric constraints. Localized mountain building was initiated during a Cretaceous microcontinent collision event in central Tibet and ocean-continent convergence in southern Tibet. Geological data indicate that India began colliding with Asian-affinity rocks 65–60 million years ago (Ma). High-elevation (>4 km) east—west mountain belts were established in southern and central Tibet by ~55 Ma and ~45 Ma, respectively. These mountain belts were separated by $\leq 2 \text{ km}$ elevation basins centred on the microcontinent suture in central Tibet, until the basins were uplifted further between ~38 and 29 Ma. Basin uplift to ≥4 km elevation was delayed along the India–Asia suture zone until ~20 Ma, along with that in northern Tibet. Delamination and break-off of the subducted Indian and Asian lithosphere were the dominant mechanisms of surface uplift, with spatial variations controlled by inherited lithospheric heterogeneities. Future research should explore why surface uplift along suture zones — the loci of the initial collision — was substantially delayed compared with the time of initial collision.

Introduction

The Tibetan Plateau is Earth's broadest and highest elevation collisional system, with a mean elevation of ~5 km north of the Indian subcontinent (Fig. 1). Plateau formation profoundly influenced Asian climate dynamics¹, development of modern-day water resources and large Asian rivers², biodiversity³ and the carbon cycle^{4,5,6} through changes in the geographical distribution of land, sea and surface topography and rock erosion and weathering. However, the mechanisms that deform the continental lithosphere and change surface elevation temporally and spatially during continental collision remain unclear. These unknowns are reflected by the ongoing debates regarding Tibetan Plateau growth during the Cenozoic India–Asia

collision.

The Tibetan Plateau is geologically heterogeneous, being composed of several adjoining terranes (Fig. 1) that collided with each other during the last ~300 million years (Myr), owing to subduction of intervening ocean basins along southward younging suture zones^{7,8,9}. These multiple subduction and collision events resulted in the formation of heterogenous lithosphere and variable histories of crustal deformation and surface elevation change across Tibet.

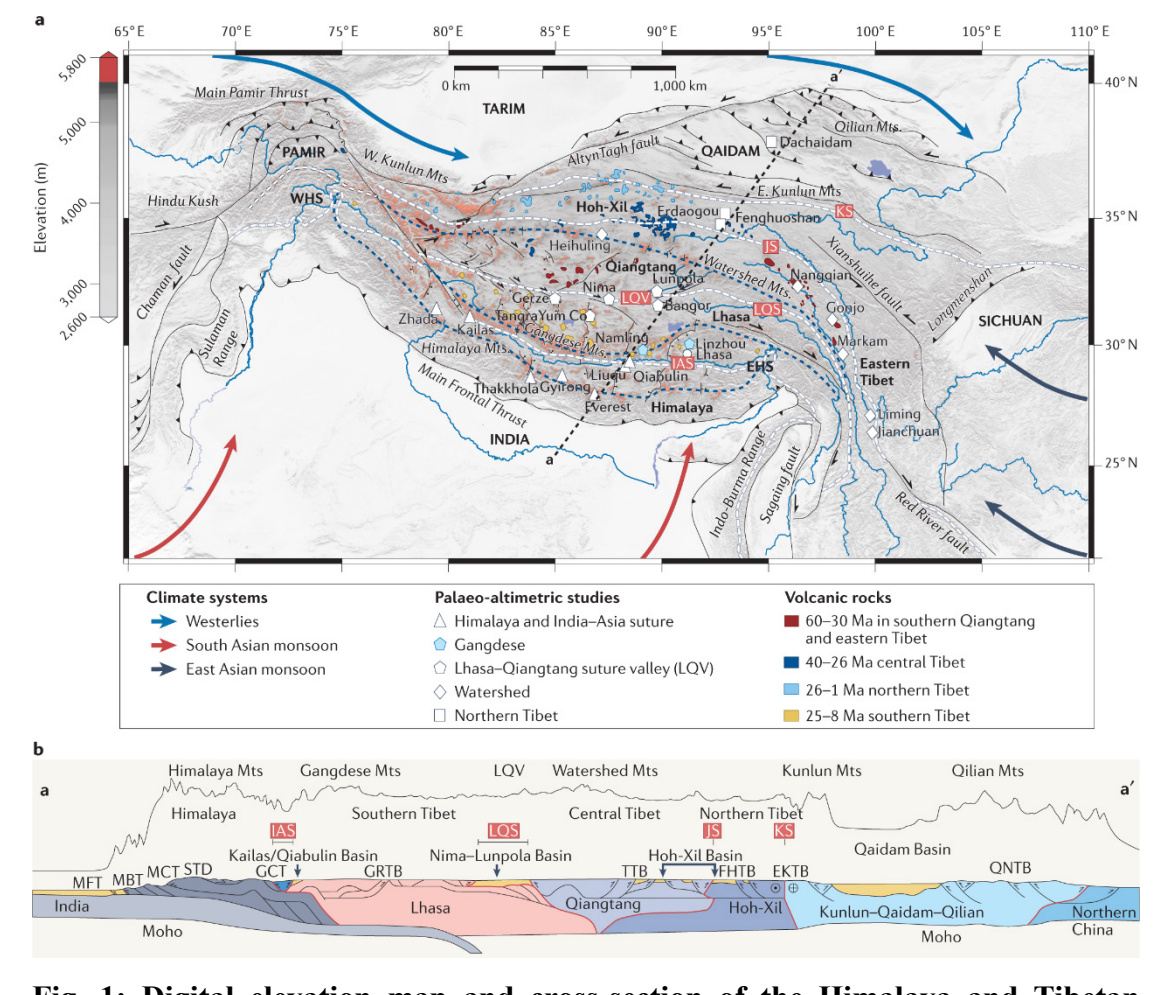


Fig. 1: Digital elevation map and cross-section of the Himalaya and Tibetan Plateau. a | Major mountain crests, terranes and sutures along with locations of palaeo-elevation reconstructions. From south to north, major terranes and mountain belts include the Himalaya terrane and Himalaya Mountains, Lhasa terrane and Gangdese Mountains in southern Tibet, Qiangtang terrane and Watershed Mountains in central Tibet, and Hoh-Xil (equivalent to Songpan-Ganzi) terrane and Kunlun Mountains in northern Tibet. Cenozoic potassic–adakitic–alkaline volcanic rocks are

most widely distributed in the vast internally drained plateau interior and systematically decrease in age southward and northward from central Tibet. Distributions of Cenozoic volcanic rocks taken from refs. 111,116,117. Present-day moisture sources for the Tibetan Plateau (bold arrows) are dominated by the South Asian monsoon, East Asian monsoon and westerlies. Better knowledge of past sources and isotopic compositions of moisture throughout the Cenozoic is critical to advancing palaeo-altimetric studies. b | Topographic profile and tectonic cross-section along the transect a-a' (north-east-south-west), displaying the geometry of main Tibetan Plateau terranes and fault zones. Mesozoic assembly of juvenile terranes in Tibet, and their bounding suture zones, strongly influenced the temporal-spatial distribution of deformation, basin development and surface elevation change during the India-Asia collision. EHS, eastern Himalayan syntaxis; EKTB, eastern Kunlun thrust belt; FHTB, Fenghuoshan-Hoh-Xil thrust belt; GCT, Great Counter Thrust; GRTB, Gangdese retroarc thrust belt; IAS, India-Asia suture; JS, Jinsha suture; KS, Kunlun suture; LQS, Lhasa-Qiangtang suture; LQV, Lhasa-Qiangtang suture valley; Ma, million years ago; MFT, Main Frontal Thrust; MBT, Main Boundary Thrust; MCT, Main Central Thrust; QNTB, Qilian-Nanshan thrust belt; STD, south Tibetan detachment; TTB, Tanggula thrust belt; WHS, western Himalayan syntaxis. Panel b adapted with permission from ref. 13, American Journal of Science.

The timing of the initial continental collision between India and Asia, which is the youngest and most drastic collision event during Tibet's assembly, is strongly debated, with estimates ranging from >65 million years ago (Ma)^{9,10} to ~25 Ma^{11,12}. The controversy over the collision time stems, in part, from the modest amount of documented upper-crustal deformation in Tibet between ~65 and 25 Ma and the proposition that a Cenozoic ocean basin could have subducted between India and Asia without leaving a definitive record in the surface geology^{12,13}. Tighter constraints on the timing of the initial India—Asia collision are critical for determining how much of the >4,000 km of convergence between India and Asia since ~60 Ma was accommodated by oceanic subduction versus deformation¹⁴ and recycling of continental lithosphere into the mantle^{15,16}, as well as the land—sea geographical

distribution through time that influenced water vapour sources and palaeoclimate¹⁷.

Tibet's temporal–spatial distribution of surface elevation change and the geodynamic mechanisms responsible are also difficult to quantify, but are necessary to assess how topographic growth impacts climate^{18,19}, biotic and ecological evolution²⁰. General perceptions are that Tibet grew outward from the India–Asia suture (IAS) since the Eocene by either Indian continental underthrusting (Fig. 2a) or oblique continental subduction^{21,22} (Fig. 2b). However, phases of regional and rapid surface uplift during the past 20 Ma in response to convective removal of mantle lithosphere have also been invoked^{1,8,23} (Fig. 2c). Furthermore, most surface uplift in eastern Tibet is purported to be <15 Ma and driven by flow of weak crust beneath it²⁴ (Fig. 2d).

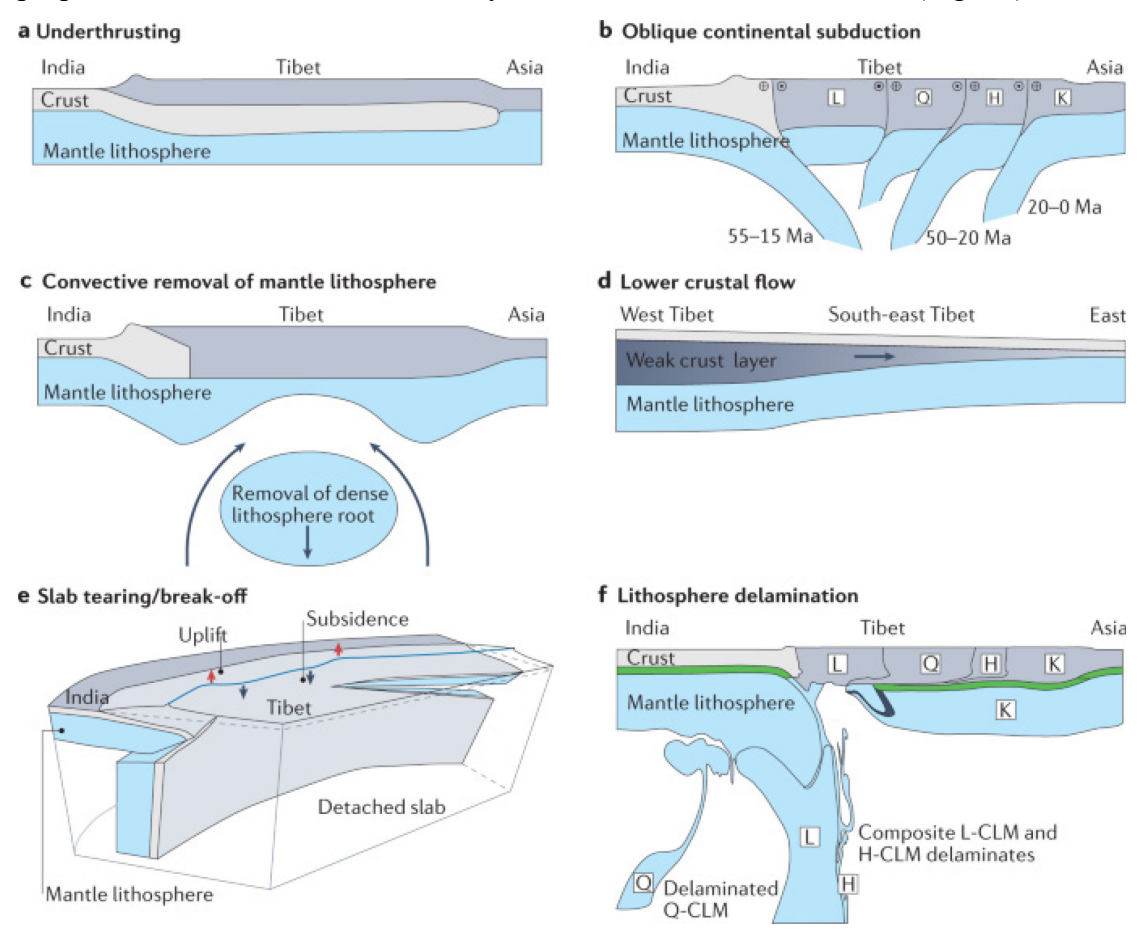


Fig. 2: Proposed geodynamic mechanisms of continental collisional deformation and plateau formation. a | Indian lithosphere subducted horizontally northward beneath the Tibetan crust²⁰⁴. b | Subduction of continental lithosphere along sutures led to stepwise northward growth of the Tibetan Plateau²¹. c | Uniform thickening of Asian lithosphere followed by removal of its dense lower lithosphere has been

suggested to result in a phase of 1.0–2.5 km of surface uplift within a few million years (Myr)¹. d | Topographically driven flow of weak lower crust could have uplifted eastern and south-eastern Tibet and has been suggested to explain the low topographic gradient from the plateau interior to Southeast Asia²⁴. e | Dynamic surface subsidence during dense slab break-off and surface uplift after slab break-off²⁷. f | Northward advancing subduction of Indian lithosphere induced thickening and delamination of the weaker Asian lithosphere²⁸. Rather than one mechanism alone, it is likely a variable combination of geodynamic mechanisms in space and time are required to explain geological evolution and growth history of the Tibetan Plateau. CLM, continental lithospheric mantle; H, Hoh-Xil terrane; K, Kunlun terrane; L, Lhasa terrane; Ma, million years ago; Q, Qiangtang terrane. Panel a adapted with permission from refs.^{204,205}, Wiley and Elsevier. Panel b adapted (to a simplified schematic, not to scale) with permission from ref.²¹, AAAS. Panel e adapted with permission from ref.²⁷, GeoScienceWorld. Panel f adapted with permission from ref.²⁸, Geological Society of America.

The accelerating generation of quantitative palaeo-altimetry data across Tibet has resolved non-uniform surface uplift histories across Tibet, with parts being uplifted to substantial elevations either earlier or later than previously speculated^{22,25,26}. These unanticipated findings, along with increasingly well-resolved temporal–spatial records of Cenozoic magmatism¹³, have promoted additional geodynamic drivers of surface elevation change, such as break-off of subducted continental slabs²⁷ (Fig. 2e) and continental lithosphere delamination²⁸ (Fig. 2f).

In this Review, we discuss Tibetan Plateau evolution and growth, and highlight the role of Cretaceous tectonism in imparting lithospheric heterogeneities in Tibet, the debates and constraints on the timing of initial India—Asia collision and the history and geodynamic mechanisms of Cenozoic surface elevation change. Major findings are that the surface uplift history was highly variable across Tibet, requiring subcrustal mechanisms such as subduction, delamination and break-off of Indian and Asian lithosphere, and was strongly influenced by lithospheric heterogeneities inherited from precursor tectonic events.

Cretaceous tectonism and surface uplift

A holistic model of Tibetan Plateau development must consider topographic and lithospheric heterogeneities in Asia that were inherited from tectonic events prior to the India–Asia collision^{9,29}. In this section, we discuss the Cretaceous events that pushed parts of Tibet above sea level and weakened its lithosphere, including the collision between the Lhasa and Qiangtang terranes in central Tibet and the development of a Cordilleran or Andean-style continental margin in southern Tibet.

Lhasa-Qiangtang collision

The collision of the Lhasa terrane with the southern margin of the Asia ~120 Ma resulted in initial growth of the Watershed Mountains³⁰ (Fig. 1). Collisional convergence occurred after northward and southward subduction of intervening Meso-Tethys oceanic lithosphere along the Lhasa–Qiangtang suture (LQS) zone³¹ (Fig. 1). Here we summarize the geological manifestations of the Lhasa–Qiangtang collision and its inferred impacts on lithospheric architecture.

Deformation and uplift above sea level by ~120 Ma in central Tibet are recorded by an angular unconformity between strongly deformed ≥150 Ma marine rocks and overlying lesser deformed ≤120 Ma non-marine volcanic and clastic rocks^{32,33}. A phase of rock cooling between 110 and 70 Ma, centred along the modern location of the Watershed Mountains (Fig. 1), suggests that deformation and erosion were protracted³⁴. The Watershed Mountains are aptly named as, at the largest scale, they form a divide between rivers that flow southward into the Indian Ocean from those that flow eastward into the Pacific Ocean. Sedimentologic studies of basins in northern Tibet³⁵ and along the LQS zone³⁶ suggest that this drainage divide is inherited from Cretaceous tectonism.

Thrusting and non-marine deposition commenced along the LQS by ~120 Ma and propagated southward into the northern Lhasa terrane after ~100 Ma^{30,37}. Foundering of Meso-Tethys oceanic lithosphere after initial Lhasa–Qiangtang collision ignited an east–west 120–105 Ma magmatic belt in the northern Lhasa and southern Qiangtang terranes³¹. Cretaceous uplift of the Watershed Mountains is attributed to northward underthrusting of Lhasa terrane lithosphere during the Lhasa–

Qiangtang collision^{30,32}.

Neo-Tethys oceanic subduction

Cretaceous convergence between the Neo-Tethys oceanic and Asian continental plates resulted in Cordilleran or Andean-style magmatism and mountain building in southern Tibet^{138,39}. Northward subduction of Neo-Tethys oceanic lithosphere beneath southern Tibet, and associated growth of the Gangdese magmatic arc, was initiated between ~240 and 190 Ma^{40,41}. Substantial mountain building did not occur until >100 Myr later, however, as most of the Lhasa terrane experienced marginal to shallow marine sedimentation prior to ~95 Ma⁴². Overlying ≤95 Ma non-marine strata record southern Tibet's rise above sea level^{43,44}. In the southern Lhasa terrane, Cretaceous strata were folded and eroded prior to deposition of overlying ~65–40 Ma non-marine volcanic-bearing strata^{38,39,45}. These geologic relationships provide unambiguous evidence for shortening and surface uplift prior to the India–Asia collision. The presence of ~65 Ma evaporites and eolianites in central Tibet suggests that the Gangdese Mountains might have served as an effective orographic barrier to Neo-Tethys Ocean moisture sources to the south³⁶.

Applications of empirically based geochemical proxies for crustal thickness to Gangdese magmatic arc rocks yield contradictory results^{46,47,48,49}. Although all suggest establishment of a moderately thick crust (~40–55 km) at ~65 Ma, the estimated crustal thicknesses variably increase^{46,48}, decrease⁴⁹ or remain steady⁴⁷ between ~90 and 65 Ma. Raising additional caution in these geochemical proxies are estimates of thick crust in the northern Lhasa terrane at ~120–105 Ma⁴⁷ when it was near or below sea level⁴².

Termination of marine deposition in northern Tibet

Non-marine sedimentary basins began to accumulate in northern Tibet by ~85 Ma⁵⁰, attesting to its rise above sea level. The youngest shallow marine strata in westernmost Tibet are ~80 Ma and record a westward marine regression⁵¹. Unlike central and southern Tibet, northern Tibet did not experience substantial Cretaceous crustal shortening or magmatism, and thus its lithosphere would have been comparatively stronger at the time India collided with Asia¹³.

Although there is evidence for Cretaceous growth of relatively narrow mountain ranges in central and southern Tibet, the magnitude of surface uplift remains to be quantified. The transformation of this pre-Cenozoic locally mountainous topography into the modern plateau topography is a result of India–Asia collision, yet confidence in the initiation age of this collision remains poor.

India-Asia suturing

Competing hypotheses for the closure history of the Neo-Tethys Ocean include the opening and closing of the oceanic Greater India Basin (Fig. 3a), collision of India with an intra-oceanic arc (Fig. 3b,c) and a single subduction-collision model (Fig. 3d). These hypotheses make contrasting predictions about the size of continental Greater India — the northern extension of the Indian subcontinent that has subducted since collision began⁵² — and the initiation age of India–Asia intercontinental collision. However, each of the models is based on the same evidence — that an early foreland basin located north of the Tethyan Himalaya and sourced from a Gangdese affinity arc loaded the subducted continental terrane at the time of the initial collision between them at 65–59 Ma⁵³. In the following sections, the constraints provided by the geology of the IAS zone followed by the motivations, implications and challenges of each of the hypotheses are summarized.

Geology of the India-Asia suture

The geology of the archetypal IAS zone in southern Tibet has been extensively investigated since the 1980s^{38,39} and must be honoured in tectonic interpretations. South of the IAS zone are Indian passive continental margin strata of the Tethyan Himalaya⁵⁴. All rock units exposed north of the Tethyan Himalaya are most simply interpreted as components of an ocean–continent convergent margin system along the southern margin of Asia^{7,38,39}. From south to north, these rock units include ~160–60 Ma subduction complex rocks, ~132–125 Ma ophiolites and overlying ~130–50 Ma forearc basin strata (the Xigaze forearc), and the >190 Ma to ~40 Ma Gangdese magmatic arc¹³. This geologic framework led to the conventional view that India collided with Asia following the northward subduction of a single Neo-Tethys oceanic plate beneath the Lhasa terrane^{38,39}. If the conventional northward subduction model

was true, then the timing of the first appearance of Asian detritus in Tethyan Himalaya strata would mark the initiation age of India–Asia collision.

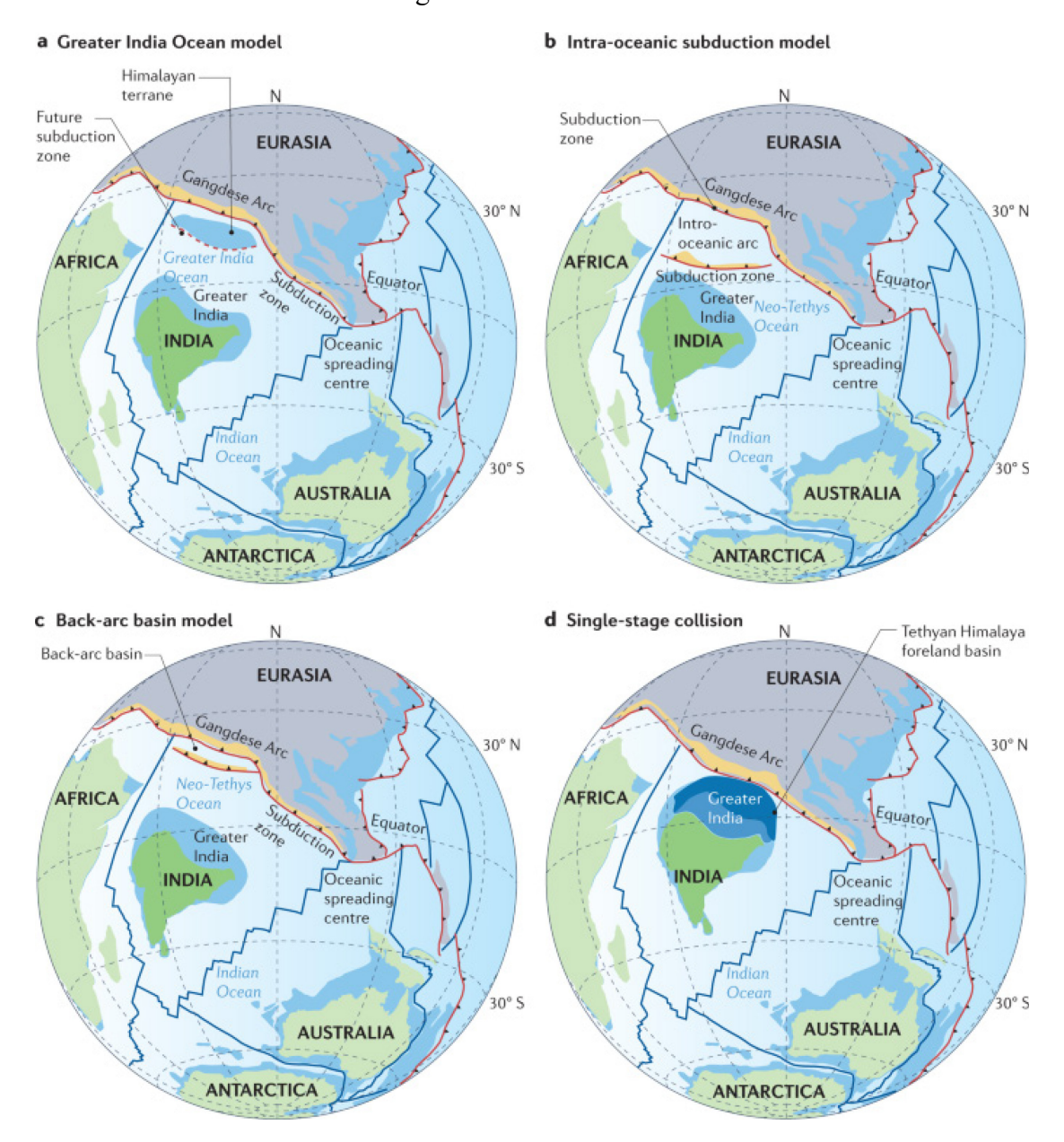


Fig. 3: Competing hypotheses for the history of India–Asia suturing. All panels represent competing palaeogeographic reconstructions at ~65 million years ago (Ma). a | Greater India Basin model in which a Himalayan terrane rifted from India during the Cretaceous and collided with Asia prior to subduction of the oceanic Greater India Basin^{12,60,61}. b | Collision of Greater India with an intra-oceanic arc that developed near the Equator, distal from the Asian margin^{11,66,67}. c | Collision of Greater India with the Xigaze forearc and arc, which rifted from the southern margin of Asia between ~90 and 70 Ma¹³. d | Single-stage collision of Greater India with a north–

south extent of \geq 2,400 km^{13,16,72}. Age of initial India–Asia collision is oldest (\geq 60 Ma) in central Himalaya–Tibet and decreases to 55–50 Ma along strike to west and east^{56,73}. Competing models have profoundly different implications for the timing of initial India–Asia collision and land–sea distribution during the early Cenozoic; none of which are yet fully supported by all available data sets.

Arc detritus appeared in a central Tethyan Himalaya collision-related foreland basin between 65 and 59 Ma^{55,56}. Arc-derived detrital zircons in Tethyan Himalayan strata are indistinguishable in age and hafnium isotope compositions from those in <85 Ma Xigaze forearc basin strata¹³. Detrital zircons in >85 Ma Xigaze forearc basin strata were, in large part, derived from isotopically evolved igneous rocks in the Lhasa terrane¹³. These findings suggest that the Xigaze forearc basin developed adjacent to the Asian continental margin and collided with the Tethyan Himalaya by 59 Ma. A conventional interpretation of these findings would be that the India–Asia collision was underway by 59 Ma, substantially earlier than the canonical 50–40 Ma age for collision initiation^{8,57}.

A compelling argument to question such an old (>59 Ma) collision is based on the convergence history between India and Asia, which is well constrained from the age of oceanic crust between continents and palaeomagnetically determined apparent polar wander paths⁵⁸. If collision occurred at ~60 Ma, Indian and Asian continental lithosphere must have absorbed an enormous amount (~4,000 km) of convergence in an entirely continental setting since. Such a large convergence magnitude is more than double the total amount of <65 Ma north–south crustal shortening that has been estimated in Asia (<1,000 km) and the Himalaya (<1,000 km)¹⁴. This crustal shortening deficit has helped fuel alternative hypotheses that involve rifting the Tethyan Himalaya from India and colliding it with Asia or having India collide with an intra-oceanic arc prior to the penultimate collision between India and Asia.

Oceanic Greater India Basin model

Motivated to resolve the crustal shortening deficit, and initially supported by

palaeomagnetically determined palaeolatitude results, is the hypothesis that a ≥ 2,000 km-wide oceanic Greater India Basin opened during Cretaceous rifting of the Tethyan Himalaya from the Indian subcontinent^{12,59,60,61} (Fig. 3a). This hypothesis is compatible with collision of the Tethyan Himalaya with Asia by 59 Ma. Closure of the oceanic Greater India Basin and the ensuing India—Asia collision might not have occurred until as recently as ~25 Ma when crustal shortening estimates in the Himalaya and Asia begin to match convergence magnitudes¹². Some of the initial supporting palaeomagnetic data, however, were shown to be compromised by remagnetization⁶². A statistically more rigorous analysis of the palaeomagnetic data also challenges their use as evidence in favour of an oceanic Greater India Basin⁶³. There is no geologic evidence that unequivocally supports the presence of such an ocean basin, whereas there is a substantial amount of geologic evidence against it, for example, stratigraphic continuity from the Tethyan Himalaya to continental India and ≤45 Ma high-grade metamorphism in the Himalaya^{13,55,64}.

Intra-oceanic arc model

Another model that reduces the crustal shortening deficit calls upon ~60 Ma collision of India with a south-facing intra-oceanic arc-trench system that developed near the Equator ^{11,65,66,67} (Fig. 3b). In this model, penultimate India—Asia collision did not occur until ~45 Ma closure of the back-arc Neo-Tethys ocean basin. The former existence of the intra-oceanic subduction zone is supported by high-velocity seismic anomalies in the lower mantle, which extend approximately north-west–south-east from beneath modern Arabia to just south of the southern tip of the Indian subcontinent ⁶⁸. Collision of India with a juvenile intra-oceanic arc that developed far south from Asia, however, cannot explain the appearance of the Xigaze forearc basin and continental Asian detritus in Tethyan Himalaya strata between 65 and 59 Ma^{10,69,70}.

A modified India–arc collision model¹³ (Fig. 3c) explains the appearance of Asian detritus in Tethyan Himalaya strata by rifting a southern portion of the Gangdese magmatic arc, along with the Xigaze forearc basin to the south, during a ~90–70 Ma phase of Neo-Tethys oceanic slab rollback. Slab rollback led to the

opening of a Japan Sea-like back-arc ocean basin and collision of the rifted Asian arc with India near the Equator by ~60 Ma. The hypothetical ~45 Ma suture in this model is located on the north side of the Xigaze forearc basin, which is everywhere bound by the south-dipping Miocene (~20 Ma) Great Counter Thrust (GCT) (Fig. 1b), or within the southernmost Gangdese magmatic arc. However, at present no direct geologic evidence exists for the opening or closing of the Xigaze back-arc basin. No Cenozoic oceanic crustal or deep marine rocks have been identified anywhere within the Himalaya or Tibet.

Single subduction-collision model

From a geologic perspective, the simplest and most conservative interpretation remains a single subduction-collision model in which India first collided with Asia in southern Tibet by 65–59 Ma^{55,56,69,71} (Fig. 3d). The single subduction-collision model requires a very large continental Greater India, with palaeomagnetically determined estimates in the range of 2,700–1,900 km⁷². The age of India–Asia collision initiation decreases to 55–50 Ma towards the western and eastern Himalayan syntaxes^{56,73,74,75} (Fig. 1). The single collision model initiating along the central IAS zone challenges a previous paradigm^{76,77} that India–Asia collision initiated in the north-western Himalaya at ~55–50 Ma and decreased in age eastward to ~38 Ma in the Indo-Burma Range (Fig. 1).

Since \sim 60 Ma, Greater Indian lithosphere has been impinging northward into and subducting beneath Asian lithosphere. A rapidly growing amount of palaeo-elevation reconstructions and geologic data demonstrates that the temporal–spatial distribution of surface uplift, magmatism and deformation was highly variable across Tibet, and highlights a strong influence of inherited lithospheric strength heterogeneities on the geodynamic evolution.

Palaeo-altimetry in Tibet

The quest to resolve Tibet's uplift history catapulted the field of palaeo-altimetry^{78,79}. Quantitative reconstructions of palaeo-elevation (Box 1, Fig. 4 and Supplementary Table 1) provide critical constraints on the timing and geodynamic mechanisms of continental deformation and plateau growth. Palaeoenvironmental

data, such as flora and fauna, proxies of temperature and isotopic composition of precipitation, and sedimentary facies and their associations, provide quantitative and qualitative constraints on palaeo-elevation. These palaeo-elevation constraints, when cross-checked with the geologic history of crustal deformation and magmatism, elucidate the geodynamic processes responsible for surface uplift.

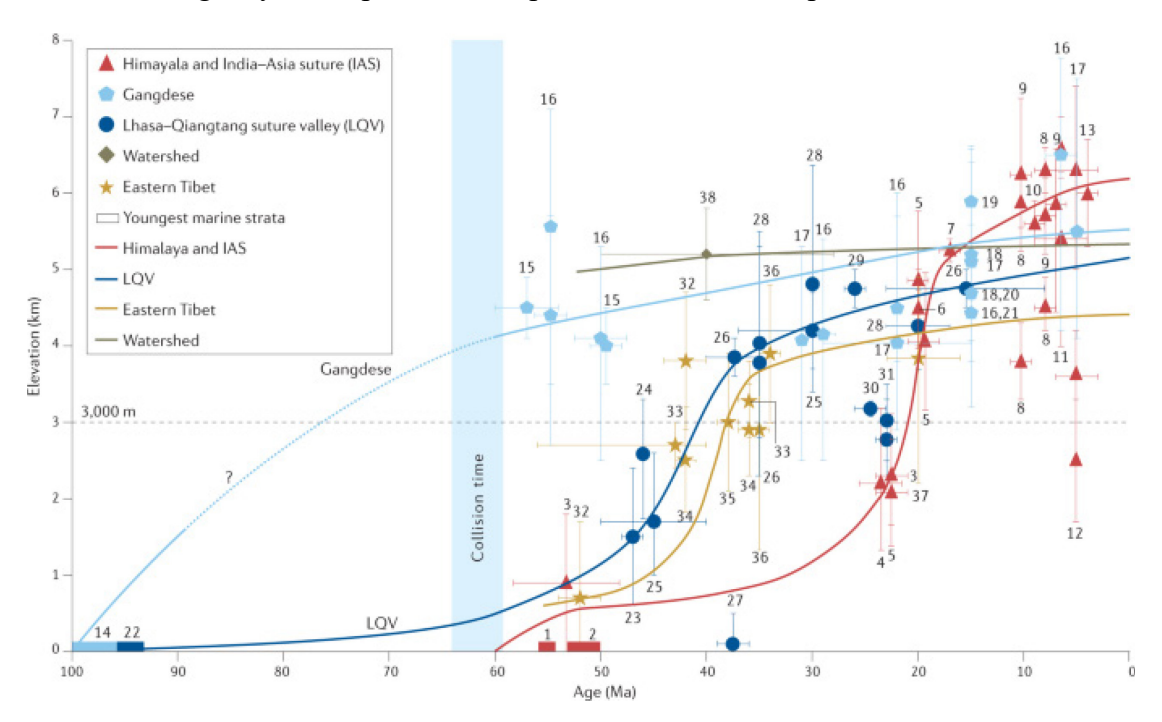


Fig. 4: History of surface elevation change across Tibet. The Himalaya and India—Asia suture (IAS) zone constrained by the youngest marine strata in the Xigaze forearc basin (~54 million years ago (Ma))^{71,105} and Tethyan Himalaya (~50 Ma^{106,107}), Liuqu, Qiabulin, Dazhuqu and Kailas basins^{101,104,150}, Mount Everest^{151,152} and Thakkhola¹⁵³ and Zhada^{154,155,156} basins. Gangdese Mountains constrained by the youngest (~95 Ma) marine strata⁴³ and Linzhou^{25,99} and Namling^{85,90,99,108,109} basins. Northern flank of Gangdese Mountains constrained by Tangra Yum Co Basin¹³³. Lhasa—Qiangtang suture valley (LQV) constrained by youngest (~95 Ma) marine strata⁴² and Bangor⁹¹, Lunpola^{22,86} and Nima¹³⁷ basins. Gerze Basin in western Lhasa—Qiangtang suture (LQS) zone might have been at low elevation until as recently as ~39 Ma⁸³. Watershed Mountains constrained by the Heihuling Basin⁹⁸. Eastern Tibet constrained by the Nangqian¹²⁵, Gonjo¹²⁶ and Markam¹²⁷ basins. References corresponding to each numbered study — Himalaya and IAS zone: 1 (ref.¹⁰⁵), 2

(refs. ^{106,107}), 3 (ref. ¹⁰⁴), 4 (ref. ²⁰⁶), 5 (ref. ¹⁵⁰), 6 (refs. ^{101,149}), 7 (refs. ^{151,152}), 8 (refs. ^{78,153}), 9 (ref. ⁷⁹), 10 (ref. ¹⁵⁴), 11 (ref. ¹⁵⁶), 12 (ref. ²⁰⁷), 13 (ref. ¹⁵⁵); Gangdese Mountains: 14 (ref. ⁴³), 15 (ref. ²⁵), 16 (ref. ⁹⁹), 17 (ref. ⁸⁵), 18 (ref. ²⁰⁸), 19 (ref. ¹⁰⁹), 20 (ref. ⁹⁰), 21 (ref. ¹¹⁰); LQV: 22 (ref. ⁴²), 23 (ref. ⁹¹), 24 (ref. ¹³³), 25 (ref. ⁸⁷), 26 (ref. ¹³⁶), 27 (ref. ⁸³), 28 (ref. ²²), 29 (ref. ¹³⁷), 30 (ref. ¹³⁸), 31 (ref. ²⁰⁹); eastern Tibet: 32 (ref. ¹²⁶), 33 (ref. ¹³¹), 34 (ref. ²¹⁰), 35 (ref. ¹²⁵), 36 (ref. ¹²⁷), 37 (ref. ²¹¹); and Watershed Mountains: 38 (ref. ⁹⁸). All data supplied in Supplementary Table 1. Available palaeo-altimetric results have large uncertainties but are generally internally consistent where available. Additional multi-proxy palaeo-altimetric investigations coupled with isotope-enabled general circulation climate models are needed to further resolve the spatio-temporal history of surface elevation change in Tibet.

Carbonates, leaf lipids (waxes) and hydrous minerals in the rock record have the potential to record surface water compositions at the time of their formation. Modern moisture in the Himalaya and southern Tibet is mostly derived from southerly Indian Ocean moisture sources and experiences strong isotope fractionation by Rayleigh distillation as a function of elevation. Southern Tibet is thus ideal for stable isotope palaeo-altimetry under the assumption that moisture sources have been similar since initial uplift of an orographic barrier to moisture, such as the Gangdese Mountains. In contrast, modern water isotopic compositions in northern Tibet are influenced by mixing of different moisture sources (for example, southerly, westerly and recycled surface water) and complex atmospheric processes, and thus do not correlate well with surface elevation^{80,81}.

Another factor to consider in stable isotope palaeo-altimetry is the extent to which primary carbonate oxygen isotope compositions are reset during sedimentary burial^{82,83} or hydrothermal perturbations⁸⁴, which can be challenging. The ideal approach is to conduct multi-proxy palaeo-altimetry and evaluate the degree of consistency among the proxies^{85,86,87}. Carbonate clumped isotope thermometry^{88,89} has potential to quantify the temperatures at which carbonates precipitated or recrystallized in the case of burial. If primary temperatures of carbonate precipitation

are obtained, they can be used to increase the precision of oxygen isotope palaeo-altimetry and as an independent palaeo-altimeter given an estimation of the past thermal lapse rate. Palaeo-elevation reconstructions based on fossil leaf characteristics (Climate Leaf Analysis Multivariate Program (CLAMP)90; (Box 1)) are also gaining importance in Tibet as vigorous exploration unearths more fossils⁹¹.

Collectively, palaeo-altimetric approaches are limited by uncertainties about past climate conditions, such as sea and land surface temperatures, sources and isotopic compositions of moisture, atmospheric circulation, isotope and thermal lapse rates, and mean annual temperature. High-resolution isotope-enabled general circulation models of modern and past climate can simulate these quantities and provide an exciting tool for advancing the field of palaeo-altimetry⁹². Idealized models that only consider uniform reductions in the elevation of the Tibetan Plateau suggest that the assumption of water isotope fractionation by Raleigh distillation is valid in monsoonal high-elevation regions but breaks down at lower elevations and under weakened monsoonal conditions^{93,94}. Nevertheless, the model trends in Tibet are towards one of less water isotope depletion with decreasing elevation, suggesting that any reconstructed highly depleted water isotopic values require high elevations.

An outstanding question is the extent to which water isotope fractionation by Rayleigh distillation operated during the earlier stages of India–Asia collision, when the Earth was in a warmer greenhouse world and the land–sea–topography distribution was drastically different. The assumption of Rayleigh distillation was invalidated by a set of Eocene (~42 Ma) specific isotope-enabled climate models of large-scale circulation in Asia⁹⁵, which indicated widespread aridity in Tibet and lateral variations in water isotope compositions, including a reversed relationship between oxygen isotope composition and elevation across Tibet's southern margin. By contrast, an Eocene simulation with a high-elevation Tibetan proto-plateau yielded water isotope compositions broadly consistent with Rayleigh distillation⁹⁶. Further inter-comparisons between different models that combine multiple proxies are needed to advance understanding of Eocene atmospheric circulation and palaeo-elevation distribution in the Himalaya–Tibetan realm⁹⁷.

It is our view that integrated isotope-enabled climate modelling and palaeo-altimetric investigations have a promising future but are currently too nascent to argue strongly for or against the assumption of water isotope fractionation by Rayleigh distillation. In the following sections, palaeo-elevation and palaeoenvironmental investigations in Tibetan basins are summarized together with other Cenozoic geological events and our geodynamic interpretations. The cited palaeo-elevations and uncertainties are those interpreted in the original studies.

India-Asia collision and surface uplift

How the Late Cretaceous locally mountainous topography of Tibet (Fig. 5a) evolved during the ~60–40 Ma stage of India–Asia collision is strongly debated. Competing hypotheses include systematic northward plateau growth from the Gangdese Mountains²², the development of a proto-plateau spanning southern and central Tibet by ~45 Ma^{30,34} and no substantial plateau by ~40 Ma⁹⁵. The studies summarized here suggest that none of these hypotheses are accurate. Instead, >4 km elevations were achieved in the Gangdese and Watershed mountains by ~55 and ~45 Ma, respectively^{25,98,99}, whereas the intervening LQS zone region remained warm, wet and at ≤2 km elevation until between ~38 and 29 Ma^{87,91,100} (Fig. 4). Interpreted geodynamic events to explain geologic and palaeo-altimetric data include break-off of the Neo-Tethys oceanic slab between 55 and 45 Ma (Fig. 5b) followed by northward underthrusting of Indian lithosphere¹⁰¹ and induced subduction^{21,102} and delamination²⁸ of Asian lithosphere between ~45 and 29 Ma (Fig. 5c,d).

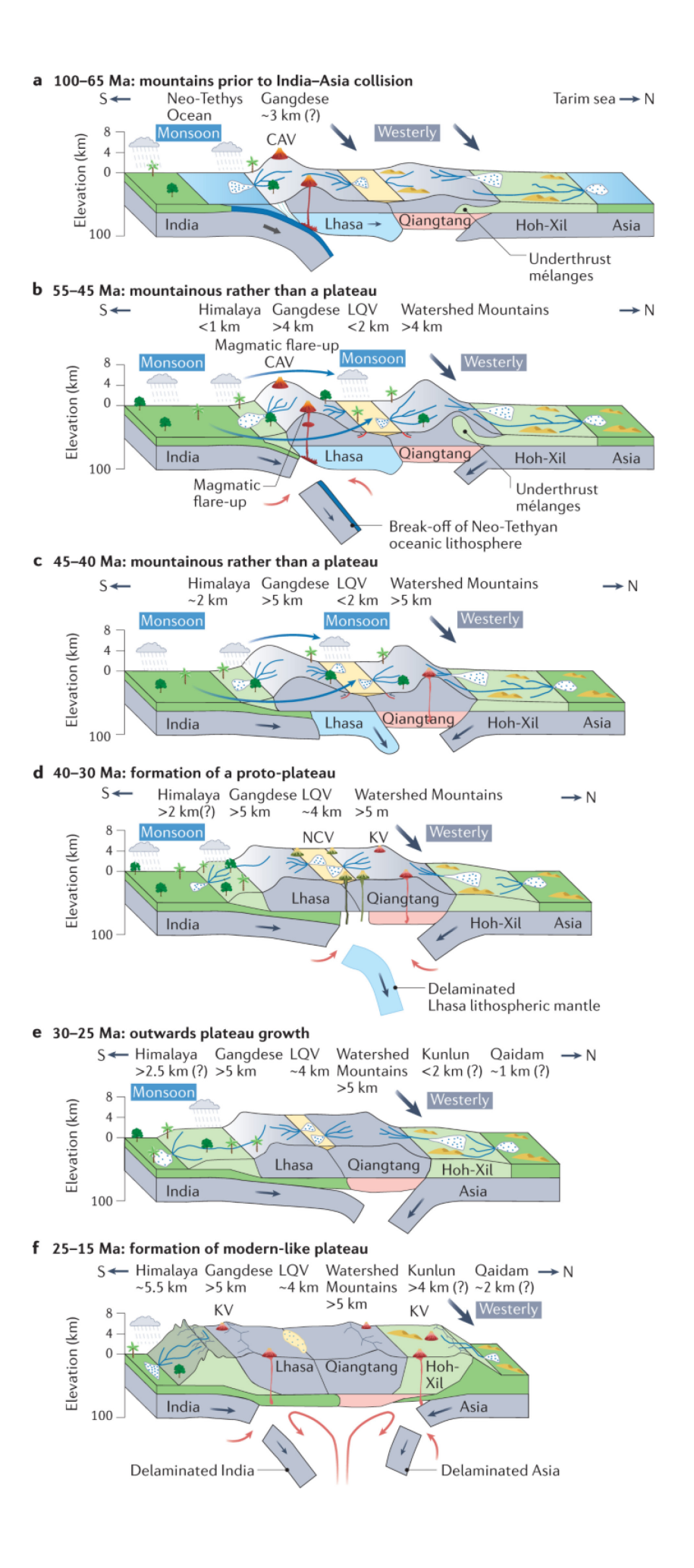


Fig. 5: Lithosphere-scale tectonic processes and corresponding changes in surface elevation and climate. a | 100-65 million years ago (Ma): northward subduction of Neo-Tethys oceanic lithosphere resulted in development of the Cordilleran or Andean-style Gangdese Mountains. b | 55–45 Ma: Neo-Tethys oceanic slab break-off resulted in magmatic flare-up and further surface uplift within Gangdese Mountains. Crustal shortening and mountain building localized in central Tibet. c | 45-40 Ma: northward underthrusting of Indian lithosphere terminated Gangdese arc magmatism and induced continental subduction along reactivated suture zones in central Tibet. Lhasa-Qiangtang suture valley (LQV) remained at low elevation with a warm monsoonal climate. d | 40-30 Ma: delamination and break-off of Lhasa terrane lithosphere and southward subduction of Asian lithosphere generated east-west belts of magmatism in central Tibet. LQV uplifted to high elevation during this time, resulting in formation of a regional proto-plateau. e | 30–25 Ma: continued northward Indian underthrusting and outward plateau growth. f | 25-15 Ma: delamination and break-off of Indian and Asian lithosphere resulted in magmatism within southern and northern Tibet, respectively, and rapid surface uplift within the Himalaya, northern Tibet and Kunlun Mountains. Black arrows indicate tectonic plate motion, blue arrows show inferred climate moisture pathways. Spatio-temporal distribution of deformation, magmatism and surface uplift across Tibet was non-uniform, implicating the importance of suture-zone reactivation and lateral variations in lithospheric strength. CAV, calc-alkaline volcanism; KV, potassium-rich volcanism; NCV, sodium-rich calc-alkaline volcanism.

Neo-Tethys slab break-off

Between ~60 and 50 Ma, the rapidly northward drifting Indian continental plate⁵⁸ subducted steeply beneath Asia¹⁰³, and the IAS zone and Tethyan Himalaya were raised above sea level but remained at low elevation104. Non-marine strata within the IAS zone (Fig. 1, Liuqu) were deposited at ~1 km elevation (Fig. 4) in a hot and wet tropical climate at ~56 Ma¹⁰⁴. The Xigaze forearc basin and central Tethyan Himalaya to the south transitioned from marine to non-marine deposition at ~54 Ma¹⁰⁵ and ~50 Ma^{55,106,107}, respectively.

The Cenozoic Linzhou and Namling basins provide archives of palaeo-elevation along the modern axis of the Gangdese Mountains (Fig. 1). The Linzhou Basin was at 4–5 km elevation between ~58 and 48 Ma based on oxygen and clumped isotope data^{25,99} (Fig. 4) and developed coeval with shortening in the Gangdese retroarc thrust belt to the north⁴⁵ (Fig. 1b). Multi-proxy results including hydrogen, oxygen and clumped isotopes show that the Namling Basin has been at ≥4 km elevation since at least ~30 Ma and might have been ~1 km higher than its modern elevation of ~4.5 km at ~15 Ma^{85,90,99,108,109,110} (Fig. 4).

Neo-Tethys slab break-off at 55-45 Ma has been interpreted to ignite a \sim 50 Ma magmatic flare-up within the Gangdese arc^{13,46,111,112} (Fig. 5b). The reduction in slab pull force due to break-off can explain the reduction in the India–Asia convergence rate from >14 cm year-1 at 55–50 Ma to <6 cm year at \sim 45 Ma^{58,113,114}, and uplift of the Gangdese Mountains to \geq 4 km elevation (Figs. 4 and 5b).

Indian underthrusting and Asian continental subduction

Following Neo-Tethys slab break-off, northward underthrusting of more buoyant Indian lithosphere terminated Gangdese arc magmatism at ~40 Ma^{101,115} (Fig. 5c). Initial collision and Indian underthrusting induced intra-continental subduction along reactivated suture zones in central Tibet^{21,102} (Fig. 5c). Approximately 46–27 Ma ultrapotassic magmatism in the northern Qiangtang terrane and sodium-rich magmatism in the southern Qiangtang terrane are attributed to southward subduction of Asian lithosphere^{102,116} and northward subduction and delamination of Lhasa terrane lithosphere^{28,117}, respectively (Fig. 5c,d). Alternatively, or in addition, Qiangtang terrane magmatism might be a manifestation of delamination or dripping of its underlying dense mantle lithosphere^{13,28}.

The syncontractional Heihuling Basin in the northern Qiangtang terrane (Fig. 1) might have been at ≥ 5 km elevation at some time between 51 and 28 Ma, based on oxygen isotope palaeo-altimetry⁹⁸ (Fig. 3). The assumption of water isotope fractionation by Rayleigh distillation is invalid in the deep interior of Tibet today⁸¹, but might have been at $\sim 50-30$ Ma when the Watershed Mountains were bounded by low-elevation regions in northern Tibet and along the LQS zone¹⁰⁰ (Fig. 5c,d). The

Watershed Mountains experienced major thrusting and folding¹¹⁸ and rapid rock cooling³⁴ between ~60 and 45 Ma, consistent with substantial surface uplift by ~45 Ma. The observation that ~46–27 Ma volcanic rocks in central Tibet are flat-lying on top of angular unconformities, together with thermochronologic evidence for limited erosion (<2 km) since ~45 Ma, suggest that low-relief (and plateau-like if at high elevation) conditions were established in central Tibet at ~45 Ma^{34,119} (Fig. 5c).

A combination of three factors can explain why crustal deformation, surface uplift and proto-plateau development were localized in central Tibet during the early stage of the India— Asia collision. The first is that central Tibet is bounded by two Mesozoic sutures (Fig.1), which are major lithospheric heterogeneities that would be prone to reactivation during subsequent collisional tectonism²¹. The second factor is that the Qiangtang terrane was underthrusted by a large volume of metasedimentary-matrix mélange when it sutured to Asia during the early Mesozoic, making it weaker than adjacent terranes^{120,121} (Fig. 5a,b). The last factor is that Watershed Mountains mark the northernmost extent of major Cretaceous tectonism and associated lithospheric weakening in Tibet¹³. Numerical geodynamic models of India—Asia collision that include lateral variations in Asian lithosphere strength, namely with central Tibet being the weakest, best simulate the non-uniform growth and complex geologic history of the Tibetan Plateau²⁸.

Surface uplift in eastern Tibet

Palaeo-altimetric studies challenge the paradigm that most surface uplift in eastern Tibet was generated by flow of crust beneath it (Fig. 2d) since the ~15 Ma onset of deep river incision^{24,122}. The ≥51 to ~37 Ma lake-dominated Nangqian Basin (Fig. 1) developed coeval with north-east–south-west shortening^{123,124}. Oxygen and clumped isotope palaeo-altimetry suggests that the Nangqian Basin region had achieved a mean elevation of ~3.0 km by ~37 Ma¹²⁵ (Fig. 4). The Gonjo Basin to the south-east (Fig. 1) evolved from an arid low-elevation (~0.7 km) basin at ~52 Ma into a high-elevation (~3.8 km) forested environment at ~42 Ma¹²⁶ (Fig. 4). CLAMP and oxygen isotope palaeo-altimetry suggest that the surface elevation of the Markam Basin increased from ~2.9 to ~3.9 km between 36 and 33 Ma¹²⁷ (Fig. 3). In the Deqin

and Weixi basins, rapid rock exhumation at $60\text{--}40\,\text{Ma}$ and syncontractional sedimentation are consistent with surface uplift initiating prior to $\sim 40\,\text{Ma}^{128,129,130}$. Near-modern elevations by $\sim 38\,\text{Ma}$ have also been reconstructed in lower elevation ($< 3.0\,\text{km}$) parts of the south-eastern Tibetan Plateau¹³¹.

The consensus among palaeo-altimetric studies is that substantial surface uplift occurred in eastern Tibet ≥ 20 Myr prior to the onset of deep river incision. This relatively early timing of surface uplift raises the possibilities that parts of eastern Tibet were characterized by internal drainage similar to that in the modern plateau interior prior to river incision³⁴ or that river incision was a response to enhanced monsoonal precipitation¹³², or both.

Lhasa-Qiangtang suture uplift and lithosphere delamination

Knowledge of the uplift history of the region between the Watershed and Gangdese mountains is critical for assessing when and how a regionally contiguous proto-plateau was established in Tibet. At the centre of this region is the LQS, which parallels a modern east—west topographic depression at ~4.5 km elevation (Fig. 1). The LQS was a topographic low relative to the Gangdese and Watershed mountains throughout the India—Asia collision, as evidenced by a series of Cenozoic basins that developed along it and within the northern Lhasa terrane^{30,32,36}. From west to east, those investigated for palaeo-altimetry include the Gerze, Tangra Yum Co, Nima, Lunpola and Bangor basins (Figs. 1 and 4).

The LQS region was at low elevation between ~50 and 39 Ma (Fig. 4). Oxygen isotope palaeo-altimetry, together with the presence of marine foraminifera, suggest that the Gerze lake basin in the west might have been near sea level until as recently as ~39 Ma⁸³. The Tangra Yum Co Basin developed along the northern flank of the Gangdese Mountains at ~2.5 km elevation between 50 and 46 Ma¹³³. The Bangor Basin to the north-east records a humid monsoonal climate and was at ~1.5 km elevation at ~47 Ma⁹¹. The age of low-elevation tropical palm and fish fossils in the Lunpola Basin was initially purported to be ~25 Ma^{26,134}, but has since been revised to ~40 Ma^{87,135}. Integrated carbonate clumped isotope thermometry and climate modelling confirm a ~1.7 km elevation of the Lunpola Basin between ~50 and

40 Ma⁸⁷. The presence of the Lhasa–Qiangtang suture valley (LQV) between the Watershed and Gangdese mountains could have permitted south-easterly monsoonal moisture-bearing winds to penetrate into central Tibet⁹¹ (Fig. 5c). However, the potentially humid ~40 Ma climate is at direct odds with isotope-enabled general circulation models that simulate arid conditions across Tibet during this time⁹⁵.

The LQV experienced ≥2 km of surface uplift between ~38 and 29 Ma⁸⁷ (Fig. 4). Assessment of extensive isotopic-based data yields palaeo-elevations of 4.5-4.7 km for the Lunpola Basin (Fig. 1) since at least ~36 Ma^{22,86,136} (Fig. 4). The Nima basin to the west was relatively dry and at near-modern elevations by 26 Ma¹³⁷ (Figs. 1 and 3). The coexistence approach on fossil pollen records, however, suggests that the Lunpola Basin could not have been higher than ~3.2 km elevation at ~25 Ma¹³⁸. Additional integrated palaeo-altimetric and climate modelling studies are needed to further explore discrepancies among different proxies and refine palaeo-elevation reconstructions^{87,139}.

Cenozoic shortening by folding and thrusting was localized along the LQS zone, but the degree of shortening is of insufficient magnitude to uplift the region from <2 km to ≥4 km elevation between ~38 and 29 Ma^{30,37}. An additional component of surface uplift is attributed to delamination of Lhasa terrane lithosphere and associated upwelling of less dense asthenosphere⁸⁷ (Fig. 5d). Delamination can explain the coeval generation of mantle-derived volcanism in the southern Qiangtang terrane and along the LQS (Fig. 1). Southward delamination of Asian lithosphere is simulated in numerical geodynamic models of the India–Asia collision that include one or more Tibetan terranes with weak lithosphere between northern Tibet and India^{28,140} (Fig. 2f).

In summary, the palaeogeography of southern and central Tibet evolved from the relatively high and narrow Gangdese and Watershed mountains at \sim 55–40 Ma into a regional proto-plateau between \sim 40 and 30 Ma. After \sim 30 Ma, the Tibetan proto-plateau began to grow outward.

Outward plateau growth

The Himalayan fold-thrust belt comprises Indian upper crust that was deformed

and thickened along the southern margin of Asia as the Greater Indian lower crust and mantle lithosphere were displaced northward beneath Tibet¹⁴¹. Consistent with intuition, numerical geodynamic models generally simulate substantial surface uplift initiating along the IAS at the time of collision initiation and propagating southward along with the Himalaya fold–thrust belt^{28,140,142}. Himalayan surface elevation change related to the downward pull and subsequent break-off of dense Indian lithosphere has also been suggested^{27,143}. In this section, we summarize unanticipated findings along the IAS zone, as well as geologic and palaeo-elevation constraints on when and how the Himalaya and northern Tibet achieved near-modern elevations.

Southward delamination and Indian slab break-off

Southward delamination and break-off of Indian lithosphere 13,27,101,117,144 (Fig. 5f) is invoked to explain onset of mantle-derived magmatism in the Lhasa terrane at \sim 26 Ma, \leq 25 Ma exhumation of Greater Himalayan continental eclogites 145,146 and \sim 25–20 Ma intrusion of leucogranites in the Himalaya 147,148 .

The surface response of slab break-off is archived in a narrow, east—west belt of ~26 to 18 Ma non-marine strata along the IAS zone (Fig. 1a, Qiabulin and Kailas). The non-marine strata rest unconformably on the southern flank of the Gangdese magmatic arc to the north and in the footwall of the south-dipping GCT to the south (Fig. 1b), which runs along the entire length of the suture in southern Tibet¹³. These strata were deposited in warm, wet and moderate (~2.3 km) to low-elevation basins that were rapidly raised to near-modern elevations between ~23 and 19 Ma^{101,104,149,150} (Fig. 4).

Indian continental slab break-off and renewed northward underthrusting triggered uplift of the Himalaya Mountains. The Mount Everest area (Fig. 1a) attained a mean elevation of >5 km by ~17 Ma (Fig. 3) based on δD values of hydrous minerals in the South Tibetan detachment (STD) (Fig. 1b) shear zone rocks^{151,152}. Oxygen isotope palaeo-altimetry of the synextensional Thakkhola and Zhada basins (Fig. 1a) suggest that the Himalaya Mountains might have been higher than their modern elevation at ~9 Ma^{153,154,155,156} (Fig. 4). It is possible that rapid ~20 Ma uplift of the Himalaya Mountains effectively blocked southerly moisture-bearing winds,

leading to further aridification in Tibet and intensification of monsoonal precipitation and rock erosion in the southern Himalaya^{104,157,158}.

Asian slab delamination and break-off

Northward delamination and break-off of the southward subducting Asian slab is inferred to generate mantle-derived volcanism in northern Tibet between ~25 and <1 Ma, and substantial surface uplift in northern Tibet and the Kunlun Mountains since ~25 Ma^{102,117} (Fig. 5f).

However, the uplift history of northern Tibet remains poorly constrained due to scarce palaeo-elevation data and uncertainties in moisture sources and processes 20,80,81 . Stable isotope palaeo-altimetric studies suggest that northern Tibet (Fig. 1, Erdaogou and Fenghuoshan) might have been at low (\leq 2 km) elevations between 72 and 37 Ma 50,159,160 . Crustal thickening by folding and thrusting between \sim 47 and 27 Ma in northern Tibet is estimated to have resulted in \leq 1.6 km of surface uplift 50,161 . The coexistence approach on a single leaf fossil and stable isotope palaeo-altimetry on \sim 17 Ma northern Tibetan strata yield conflicting results ranging from 1.4–2.9 km 162 to near-modern elevations 80,136 .

Collectively, palaeo-elevation constraints suggest that northern Tibet was likely uplifted from moderate to high elevations after 27 Ma. The presence of vast and undeformed ~24–14 Ma lake basins in northern Tibet¹⁶³ requires that surface uplift occurred by inflow of buoyant lower crust or sinking of dense lithosphere such as by northward delamination (Fig. 5f), or some combination of the two¹⁶¹.

The comparable stratigraphy and sedimentary provenance of the northern Tibetan and Qaidam basins suggest that these basins were contiguous from ~65 to 25 Ma^{35,164,165}. The presence of a large composite Tibetan–Qaidam basin implies that substantial surface uplift of the intervening Kunlun Mountains occurred after ~25 Ma, which is supported by thermochronologic records of accelerated rock cooling since ~25 Ma^{166,167}. Post-25 Ma rapid uplift and exhumation of the Kunlun Mountains are tentatively attributed to break-off of the Asian slab (Fig. 5f).

In summary, a vast and contiguous modern-like Tibetan Plateau, from the Himalaya Mountains in the south to the Kunlun Mountains to the north, was

established after ~25 Ma and likely by ~15 Ma.

Present-day Indian underthrusting

Break-off of the leading, dense part of the Indian slab (Fig. 2e) permitted renewed northward underthrusting of India at $20-15 \,\mathrm{Ma^{13,27,101}}$ (Fig. 6). Indian underthrusting can explain major $\sim\!15 \,\mathrm{Ma}$ geologic events in Tibet and heralds the final chapter in the tectonic evolution of the plateau.

Mantle-derived magmatism peaked at ~15 Ma in southern Tibet in response to accelerated removal and partial melting of Asian lithosphere as India converged northward¹³. Northward insertion and duplexing of Indian crust thickened Tibet's crust to the extent that it started collapsing eastward under its own weight, as manifested by approximately north–south trending rifting in the northern Himalaya and southern Tibet from 13 ± 3 Ma to today^{13,168,169} (Fig. 1a). The termination of volcanism in southern Tibet by 8 Ma is explained well by underthrusting of relatively cold Indian lithosphere¹¹¹ (Fig. 6). Northward insertion of Indian crust also helped drive the northward and eastward flow of weak lower crust needed to thicken the crust to modern levels in northern and eastern Tibet^{24,161}.

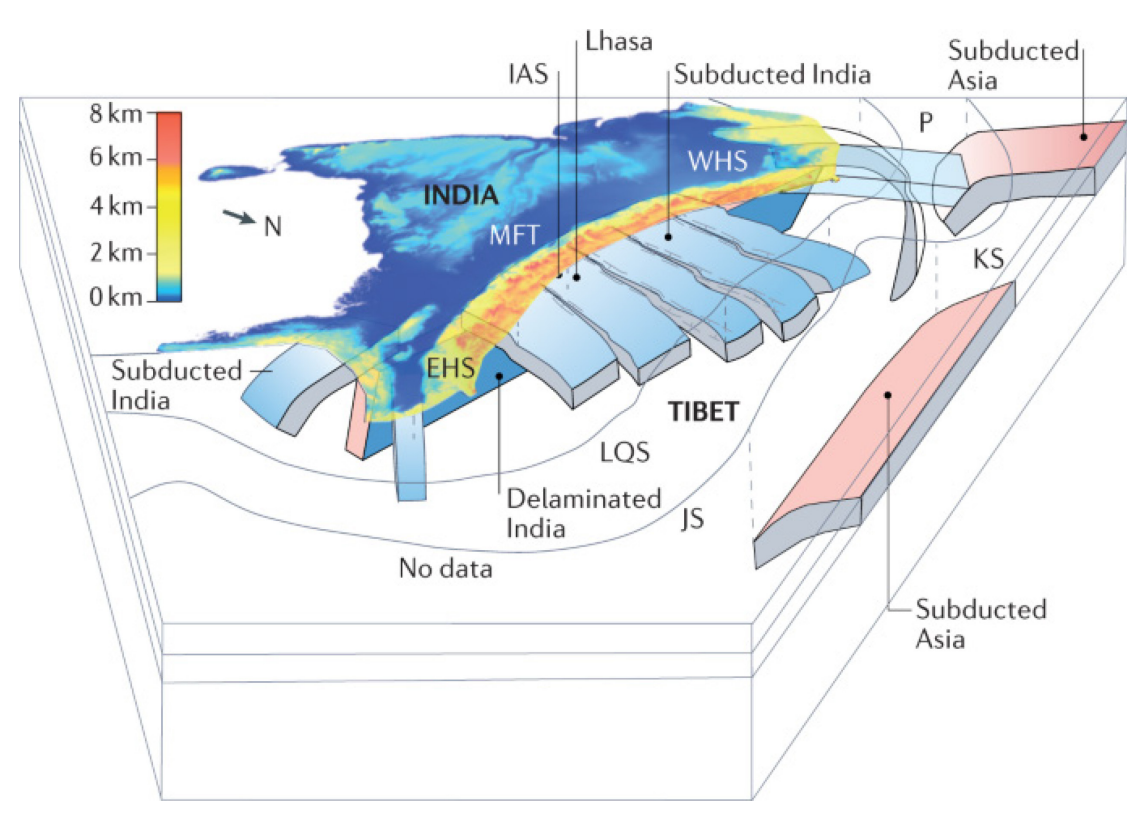


Fig. 6: Modern geometries of subducting Indian and Asian lithosphere.

Geophysical images vary widely among studies but are suggestive of substantial lateral variations in modern behaviours of Indian and Asian lithosphere. From east to west, Indian lithosphere is underthrusting Tibet at an increasingly shallower angle and extends progressively farther to the north. Onset of east—west extension across north—south rifts (dashed lines) in northern Himalaya and southern Tibet is attributed to northward underthrusting of Indian lithosphere. The rifts might have preferentially formed above north—south vertical tears in underthrust Indian lithosphere. EHS, eastern Himalayan syntaxis; IAS, India—Asia suture; JS, Jinsha suture; KS, Kunlun suture; LQS, Lhasa—Qiangtang suture; MFT, Main Frontal Thrust; P, Pamir; WHS, western Himalayan syntaxis. Figure adapted from ref.²¹², Springer Nature Limited.

Although some geophysical images indicate the Indian lithosphere to be underthrusting beneath Tibet and as far north as the LQS^{170,171,172,173} (Fig. 6), others image it to be subducting more steeply northward^{174,175,176}. There is a general consensus, however, that the Indian lithosphere is underthrusting beneath Tibet at an increasingly steeper angle from western to eastern Tibet^{173,174}. Underthrust Indian lithosphere might also be deformed by north–south-oriented vertical tears^{177,178,179} (Fig. 6), which, if present, could complicate seismic resolution. Images of southward subduction of Asian lithosphere beneath the Tibetan Plateau^{180,181,182}, or lack thereof, are similarly variable.

There are major along-strike differences in the modern behaviours of Indian and Asian lithosphere. For example, the Hindu Kush–Pamir (Fig. 1) exhibits globally unique discrete zones of intermediate-depth (down to ~300 km) earthquakes¹⁸³. Indian lithosphere is subducting nearly vertically northward beneath the Hindu Kush to ≥ 550 km depth, whereas Asian lithosphere is displaced south-eastward beneath the Pamir^{183,184,185} (Fig. 6). East of the Hindu Kush, Indian lithosphere has underthrust ~400 km northward beneath the Pamir whereas Asian lithosphere to the north delaminates northward because of India's northward impingement^{184,186} (Fig. 6).

Due to the northward motion of the Indian Plate, broken-off portions of the Neo-Tethys oceanic and Indian continental slabs are located beneath the Indian subcontinent and have been imaged using seismic tomography^{68,187}. The Neo-Tethys

slab is in the lower mantle beneath the southern Indian subcontinent, roughly along a line that connects the modern Makran and Sumatran subduction zones. If the slab sank vertically into the mantle, this line provides an estimate for where the southern edge of the Asian active continental margin was located prior to the India–Asia collision. Seismic tomography has imaged the Indian slab to be overturned (dipping to the south) in the mid-mantle beneath the northern Indian subcontinent^{68,187} (Fig. 6).

Properties of the Tibetan lithosphere show substantial spatial variations. Crustal thickness is >70 km, reaching up to 85–90 km in western and southern Tibet and decreases northward to 60–70 km in central Tibet^{170,172,180,188}. The lower part of the thick crust of southern Tibet is eclogitized^{172,189,190,191}. The thinner crust in central and northern Tibet is underlain by a hotter, partially molten uppermost mantle as indicated by lower seismic-wave velocities and stronger seismic anisotropy^{170,192,193,194}. Depth estimates to the lithosphere–asthenosphere boundary beneath central Tibet vary from ~200 km¹⁸¹ to ~100 km^{173,195}. High-velocity anomalies sitting on top of and within the mantle transition zone beneath the southern Qiangtang and Lhasa terranes are interpreted to be composed of Asian mantle lithosphere that was removed from beneath central and northern Tibet¹⁹⁶.

In summary, there is geophysical evidence for a wide variety of geodynamic behaviours of converging continental lithosphere, including sub-horizontal underthrusting to steep subduction, slab tearing and break-off, and delamination. Similar processes are called upon throughout the Cenozoic India—Asia collision to explain the non-uniform temporal—spatial distribution of deformation, magmatism and surface uplift in Tibet (Fig. 5).

Summary and future perspectives

Since the 1980s, the Tibetan Plateau evolved from a mysterious frontier to one of the most investigated orogens on Earth. Geologic and surface uplift histories are being resolved at the million-year timescale in places and require more complicated geodynamic scenarios than originally inferred.

Cretaceous tectonism weakened the southern and central Tibetan lithosphere relative to the northern Tibetan lithosphere. Suture zones are also lithospheric

heterogeneities as they localized deformation and basin development within the wide zone of the India–Asia collision; however, the surface uplift of the suture zones to high elevations was substantially delayed (by \geq 40 Myr) with respect to the timing of the initial collisions along them. The Tibetan Plateau did not rise as a single entity, nor did it rise progressively outward from the IAS, because of lithospheric heterogeneities inherited from precursor tectonic events.

Sediments of Asian continental affinity appeared in central Tethyan Himalaya collisional foreland basin strata by 59 Ma. Geologic records of ~60–40 Ma orogenesis in both Tibet and the Himalaya^{13,69} and the absence of ≤60 Ma oceanic lithosphere or ocean plate stratigraphy are consistent with the appearance of Asian sediment marking the initial India–Asia collision. A large amount of the required convergence since collision initiation, however, remains unaccounted for.

The Gangdese Mountains were at >4 km elevation and helped drive a monsoonal climate by ~55 Ma. The Watershed Mountains were established as a drainage divide during the Cretaceous and were uplifted to high elevation by ~45 Ma. Parts of eastern Tibet were uplifted to ≥3 km elevation before ~30 Ma. The LQS and IAS zones were warm, wet and at low elevation before their rise to near-modern elevations between ~38 and 29 Ma and ~23 and 19 Ma, respectively. Northern Tibet experienced magmatism but no major upper-crustal deformation during its <25 Ma rise to high elevation.

Crustal shortening and lower crust flow contributed to crustal thickening in Tibet, but subcrustal processes are equally or more important in building the plateau. Subduction, delamination and break-off of Indian and Asian lithosphere can explain the non-uniform temporal—spatial distribution of deformation, magmatism and surface elevation change across Tibet. The lower plates of suture zones might be kept at low elevation when they are attached to a dense subducting slab and get rapidly uplifted to high elevation after slab break-off. Large collisional systems recycle enormous volumes of continental lithosphere into the deeper mantle.

All current India-Asia suturing models have weaknesses. The community must

continue to seek more certainty, such as if a \leq 60 Ma oceanic basin existed between India and Asia, it is possible that scraps of it will be found, either in situ, as erosional remnants in the sedimentary record, or as xenoliths.

The history of Cenozoic upper-crustal deformation is poorly constrained for much of Tibet, making comparisons between crustal shortening and plate convergence histories tenuous. Progress is predicated upon more rigorous geologic mapping, age control on deformation and sedimentation, and construction of cross-sections.

Palaeo-elevation estimates are lacking in Tibet over large areas and time intervals. For example, high-grade metamorphism at ~45–25 Ma within the Tethyan and High Himalaya imply crustal thickening^{13,145}, but no palaeo-elevation estimates are available in this region for this time. Given uncertainties in past land–sea–topography distributions, thermal lapse rates and atmospheric circulation, further advancements in palaeo-altimetry will require integration with time-specific and geologically robust isotope-enabled general circulation models⁹².

Whether the present-day Tibetan Plateau is rising or falling remains to be demonstrated. Palaeo-altimetric studies suggest that the Gangdese and Himalayan mountains were up to 1 km higher in elevation during the Miocene (Fig. 3), implying that east—west extension thinned the crust. This 1 km decrease in elevation contradicts inferences that southern Tibet's surface elevation is in a steady state or increasing based on palaeo-crustal thickness estimates⁴⁹, Global Positioning System data197 and models attributing extension to an influx of Indian crust¹⁶⁹.

The modern architecture of the mantle beneath Tibet, such as the geometries of subducted or delaminated continental lithosphere, remains ambiguous. Additional geophysical imaging of the mantle is much needed to illuminate the processes and volume of continental lithosphere recycling. Analysis of data generated during previous and future seismic experiments across Tibet^{198,199} has the potential to reveal crustal shortening and sutures for which there is no rock record at the surface²⁰⁰, along with rheology and mechanisms of continental lithosphere deformation more broadly.

An exciting avenue of future research, afforded by geologically consistent numerical geodynamic simulations and seismic images of subducted and/or sunken lithosphere, is exploring how large continental collisions both influence and are influenced by tectonism along adjacent plate boundaries^{201,202} and by global-scale mantle convection²⁰³.

Acknowledgements

This work was supported by the Second Tibetan Plateau Scientific Expedition and Research Program (Grant No. 2019QZKK0708), the National Natural Science Foundation of China BSCTPES project (Grant No. 41988101), the Chinese Academy of Sciences (XDA20070301) and the National Science Foundation of the United States (OISE-1545859 and EAR-2048656). The authors thank L. Bai, L. Zhang, H. Zhang and F. Ping for assistance with figure preparation.

Glossary

Tibetan Plateau

The vast high-elevation plateau extending north of the Himalayan Mountains.

Terranes

Fault-bounded crustal fragments, or composites of crustal fragments, with a distinctive geological history.

Suture zones

Locations at the surface where a former oceanic basin subducted and disappeared between two terranes.

Initial continental collision

The time of final disappearance of oceanic lithosphere at the surface between two converging continents, equivalent to the time when a continent enters the trench.

Eastern Tibet

Referred to here as any part of the physiographic Tibetan Plateau that extends east of the eastern Himalayan syntaxis (EHS).

Delamination

Peeling away (downward) of dense mantle lithosphere from the overlying crust.

Rayleigh distillation

The heavy isotopes of precipitation are successively removed from the vapour as it

condenses with rising elevation.

Thermal lapse rate

The change in surface temperature with elevation; can be divided into dry adiabatic, saturated adiabatic, environmental and terrestrial lapse rates.

Box 1 Quantitative palaeo-altimetric techniques and uncertainties

Geoscientists are advancing a growing number of techniques to quantitatively reconstruct continental surface elevation back through time. To better quantify the palaeo-elevation, integration of multi-proxy stable isotope and fossil-based palaeo-altimeters and geological data is recommended.

Stable isotopes of water

Oxygen stable isotopes from carbonates and hydrogen stable isotopes from leaf lipid n-alkanes and hydrous minerals record meteoric water compositions. At increasing elevations, decreasing temperatures cause condensation of atmospheric water vapour to form precipitation (rain or snow), preferentially removing heavy isotopes (18 O and D). Palaeo-elevation is constrained from empirical and theoretical modelling of the systematic decrease in δ^{18} O and D of precipitation versus elevation 78,79 . In regions dominated by Rayleigh distillation, 2σ uncertainties derived from stable isotope palaeo-altimetry range from ~ 0.3 to ~ 1.1 km 131,213 .

Climate Leaf Analysis Multivariate Program (CLAMP)

CLAMP is a statistical method that decodes climatic signals (mean annual temperature, precipitation, enthalpy and so on) of 31 leaf characteristics represented in the physiognomy of woody dicotyledonous plants^{214,215}. The moist static energy of an air mass, consisting of moist enthalpy and potential energy, remains constant as it traverses a mountain region, hence elevation can be calculated from the difference in enthalpies between the site of interest and sea level:

$$h=H+gZ$$

Z= (Hsea level-Hunknown elevation)/g

h is moist static energy, H is enthalpy, g is gravitational acceleration. Uncertainty in elevation for CLAMP with more than 20 morphotypes of leaves is $\sim 0.9 \text{ km}^{215}$.

Glycerol dialkyl glycerol tetraethers

Glycerol dialkyl glycerol tetraethers (GDGTs) are lipid molecules from microbial membranes that correlate with temperature 216,217 . The use of GDGTs to calculate palaeo-elevation relies on an understanding of the overland thermal lapse rate and sea level temperature in the past. The 1σ uncertainty of GDGTs is 2-5 °C or ~ 0.4 to ~ 1.1 km.

Carbonate clumped isotope thermometry

 Δ 47 values of CO₂ from dissolved carbonate (enrichment of $^{13}\text{C}^{18}\text{O}^{16}\text{O}$ isotopes relative to the random distribution of heavy isotopes) are measured to determine the carbonate formation temperature, which in turn can be used to calculate the $\delta^{18}\text{O}$ value of palaeo-water^{88,89}. Carbonate clumped isotope thermometry is applied in two ways, first through changes in mean annual temperature relative to overland thermal lapse rate²¹⁸ and, second, through oxygen isotope palaeo-altimetry²¹⁹. Typical 1σ uncertainty is 2–5 $^{\circ}$ C with \geq 3 replicates per sample.

The coexistence approach

Fossil flora and fauna are assigned to their nearest living relatives to constrain palaeoclimate parameters (temperature, precipitation, relative humidity and so on) to an interval in which all nearest living relatives coexist²²⁰. Palaeo-elevation can be estimated after calibrating the effects of temperature difference and thermal lapse rate^{138,206}. Uncertainty in the coexistence approach depends on determination of nearest living relatives and their existent climate condition and thermal lapse rate.

References

- Molnar, P., England, P. & Martinod, J. Mantle dynamics, uplift of the Tibetan Plateau, and the India monsoon. *Rev. Geophys.* **31**, 357-396 (1993).
- 2 Clark, M. K. *et al.* Surface uplift, tectonics, and erosion of eastern Tibet from large-scale drainage patterns. *Tectonics* **23**, TC1006 (2004).
- Spicer, R. A. Tibet, the Himalaya, Asian monsoons and biodiversity In what ways are they related? *Plant Diversity* **39**, 233-244 (2017).
- 4 Raymo, M. E. & Ruddiman, W. F. Tectonic forcing of late Cenozoic climate. *Nature* **359**, 117-122 (1992).
- 5 Gaillardet, J. & Galy, A. Himalaya-carbon sink or source? Science 320, 1727-1728 (2008).
- 6 Guo, Z., Wilson, M., Dingwell, D. B. & Liu, J. India-Asia collision as a driver of atmospheric CO₂

- in the Cenozoic. Nat. Commun. 12, 3891 (2021).
- 7 Allègre, C. J. *et al.* Structure and evolution of the Himalaya-Tibet orogenic belt. *Nature* **307**, 17-22 (1984).
- Dewey, J. F., Shackleton, R. M., Chang, C. F. & Sun, Y. Y. The Tectonic Evolution of the Tibetan Plateau. *Philos. Trans. Royal Soc. A.* **327**, 379-413 (1988).
- 9 Yin, A. & Harrison, T. M. Geologic Evolution of the Himalayan-Tibetan Orogen. *Annu. Rev. Earth Planet. Sci.* **28**, 211-280 (2000).
- Cai, F. L., Ding, L. & Yue, Y. H. Provenance analysis of upper Cretaceous strata in the Tethys Himalaya, southern Tibet: Implications for timing of India-Asia collision. *Earth Planet. Sci. Lett.* **305**, 195-206 (2011).
- Aitchison, J. C., Ali, J. R. & Davis, A. M. When and where did India and Asia collide? *J. Geophys. Res.* **112**, B05423 (2007).
- van Hinsbergen, D. J. *et al.* Greater India Basin hypothesis and a two-stage Cenozoic collision between India and Asia. *Proc. Natl. Acad. Sci. U. S. A.* **109**, 7659-7664 (2012).
- Kapp, P. & DeCelles, P. G. Mesozoic-Cenozoic geological evolution of the Himalayan-Tibetan orogen and working tectonic hypotheses. *Am. J. Sci.* **319**, 159-254 (2019).
- van Hinsbergen, D. J. J. *et al.* Restoration of Cenozoic deformation in Asia and the size of Greater India. *Tectonics* **30**, TC5003 (2011).
- Replumaz, A., Negredo, A. M., Guillot, S., van der Beek, P. & Villasenor, A. Crustal mass budget and recycling during the India/Asia collision. *Tectonophysics* **492**, 99-107 (2010).
- Ingalls, M., Rowley, D. B., Currie, B. S. & Colman, A. S. Large-scale subduction of continental crust implied by India-Asia mass-balance calculation. *Nat. Geosci.*, 848-853 (2016).
- Roe, G. H. *et al.* A modeling study of the response of Asian summertime climate to the largest geologic forcings of the past 50 Ma. *J Geophys Res-Atmos* **121**, 5453-5470 (2016).
- An, Z., Kutzbach, J. E., Prell, W. L. & Porter, S. C. Evolution of Asian monsoons and phased uplift of the Himalaya-Tibetan plateau since Late Miocene time. *Nature* **411**, 62-66 (2001).
- Molnar, P., Boos, W. R. & Battisti, D. S. Orographic controls on climate and paleoclimate of Asia: Thermal and mechanical roles for the Tibetan Plateau. *Annu. Rev. Earth Planet. Sci.* **38**, 77-102 (2010).
- Spicer, R. A. *et al.* The topographic evolution of the Tibetan Region as revealed by palaeontology. *Palaeoeio. Palaeoenv.*, 213–243 (2020).
- Tapponnier, P. *et al.* Oblique stepwise rise and growth of the Tibet plateau. *Science* **294**, 1671-1677 (2001).
- Rowley, D. B. & Currie, B. S. Palaeo-altimetry of the late Eocene to Miocene Lunpola basin, central Tibet. *Nature* **439**, 677-681 (2006).
- 23 Harrison, T. M., Copeland, P., Kidd, W. S. F. & Yin, A. Raising Tibet. *Science* **255**, 1663-1670 (1992).
- Royden, L. H., Burchfiel, B. C. & Van der Hilst, R. D. The geological evolution of the Tibetan Plateau. *Science* **321**, 1054-1058 (2008).
- Ding, L. *et al.* The Andean-type Gangdese Mountains: Paleoelevation record from the Paleocene-Eocene Linzhou Basin. *Earth Planet. Sci. Lett.* **392**, 250-264 (2014).
- Su, T. et al. No high Tibetan Plateau until the Neogene. Sci. Adv. 5, eaav2189 (2019).
- Webb, A. A. G. *et al.* The Himalaya in 3D: Slab dynamics controlled mountain building and monsoon intensification. *Geosphere* **9**, 637-651 (2017).

- 28 Kelly, S., Beaumont, C. & Butler, J. P. Inherited terrane properties explain enigmatic post-collisional Himalayan-Tibetan evolution. *Geology* **48**, 8-14 (2020).
- 29 Molnar, P. & Tapponnier, P. A possible dependence of tectonic strength on the age of the crust in Asia. *Earth Planet. Sci. Lett.* **52**, 107-114 (1981).
- Kapp, P., DeCelles, P. G., Gehrels, G. E., Heizler, M. & Ding, L. Geological records of the Lhasa-Qiangtang and Indo-Asian collisions in the Nima area of central Tibet. *Geol. Soc. Am. Bull.* **119**, 917-933 (2007).
- Zhu, D.-C. *et al.* Assembly of the Lhasa and Qiangtang terranes in central Tibet by divergent double subduction. *Lithos* **245**, 7-17 (2016).
- Kapp, P., Yin, A., Harrison, T. M. & Ding, L. Cretaceous-Tertiary shortening, basin development, and volcanism in central Tibet. *Geol. Soc. Am. Bull.* **117**, 865-878 (2005).
- Ma, A. *et al.* The disappearance of a Late Jurassic remnant sea in the southern Qiangtang Block (Shamuluo Formation, Najiangco area): Implications for the tectonic uplift of central Tibet. *Palaeogeogr. Palaeoclimatol. Palaeoecol.* **506**, 30-47 (2018).
- Rohrmann, A. *et al.* Thermochronologic evidence for plateau formation in central Tibet by 45 Ma. *Geology* **40**, 187-190 (2012).
- Li, L., Garzione, C. N., Pullen, A., Zhang, P. & Li, Y. Late Cretaceous-Cenozoic basin evolution and topographic growth of the Hoh Xil Basin, central Tibetan Plateau. *Geol. Soc. Am. Bull.* **130**, 499-521 (2018).
- DeCelles, P. G., Kapp, P., Ding, L. & Gehrels, G. E. Late Cretaceous to middle Tertiary basin evolution in the central Tibetan plateau: Changing environments in response to tectonic partitioning, aridification, and regional elevation gain. *Geol. Soc. Am. Bull.* **119**, 654-680 (2007).
- Volkmer, J. E., Kapp, P., Guynn, J. H. & Lai, Q. Cretaceous-Tertiary structural evolution of the north central Lhasa terrane, Tibet. *Tectonics* **26**, TC6007 (2007).
- Tapponnier, P. *et al.* The Tibetan side of the India-Eurasia collision. *Nature* **294**, 405-410 (1981).
- Burg, J. P. & Chen, G. M. Tectonics and structural zonation of southern Tibet, China. *Nature* **311**, 219-223 (1984).
- Ji, W.-Q., Wu, F.-Y., Chung, S.-L., Li, J.-X. & Liu, C.-Z. Zircon U-Pb geochronology and Hf isotopic constraints on petrogenesis of the Gangdese batholith, southern Tibet. *Chem. Geol.* **262**, 229-245 (2009).
- Wang, C. et al. Petrogenesis of Middle-Late Triassic volcanic rocks from the Gangdese belt, southern Lhasa terrane: Implications for early subduction of Neo-Tethyan oceanic lithosphere. *Lithos* **262**, 320-333 (2016).
- BouDagher-Fadel, M. K. *et al.* Foraminiferal biostratigraphy and palaeoenvironmental analysis of the mid-Cretaceous limestones in the southern Tibetan Plateau. *J. Foraminiferal Res.* **47**, 188-207 (2017).
- Leier, A. L., DeCelles, P. G., Kapp, P. & Ding, L. The Takena Formation of the Lhasa terrane, southern Tibet: The record of a Late Cretaceous retroarc foreland basin. *Geol. Soc. Am. Bull.* **119**, 31-48 (2007).
- Sun, G., Hu, X., Sinclair, H. D., BouDagher-Fadel, M. K. & Wang, J. Late Cretaceous evolution of the Coqen Basin (Lhasa terrane) and implications for early topographic growth on the Tibetan Plateau. *Geol. Soc. Am. Bull.* **127**, 1001-1020 (2015).

- 45 Kapp, P. et al. The Gangdese retroarc thrust belt revealed. GSA Today 17, 4-9 (2007).
- Zhu, D.-C., Wang, Q., Cawood, P. A., Zhao, Z.-D. & Mo, X.-X. Raising the Gangdese Mountains in southern Tibet. *J. Geophys. Res. Solid Earth* **122**, 214-223 (2017).
- Hu, F. *et al.* Quantitatively tracking the elevation of the Tibetan Plateau since the Cretaceous: Insights from whole-rock Sr/Y and La/Yb ratios. *Geophys. Res. Lett.* **47**, e2020GL089202 (2020).
- Tang, M., Ji, W.-Q., Chu, X., Wu, A. & Chen, C. Reconstructing crustal thickness evolution from europium anomalies in detrital zircons. *Geology* **49**, 76-80 (2021).
- 49 Sundell, K. E., Laskowski, A. K., Kapp, P. A., Ducea, M. N. & Chapman, J. B. Jurassic to Neogene quantiative crustal thickness estimates in southern Tibet. *GSA Today*, 4-10 (2021).
- Staisch, L. M. *et al.* A Cretaceous-Eocene depositional age for the Fenghuoshan Group, Hoh Xil Basin: Implications for the tectonic evolution of the northern Tibet Plateau. *Tectonics* **33**, 281-301 (2014).
- Sha, J., Fabbi, S., Cestari, R. & Consorti, L. Stratigraphic and taxonomic considerations on the Late Cretaceous rudist fauna of Aksai Chin (Western Tibet, China) from the De Filippi Collection. *Carnets Geol.* **20**, 249-272 (2020).
- 52 Ali, J. R. & Aitchison, J. C. Greater India. *Earth-Sci. Rev.* **72**, 169-188 (2005).
- Ding, L. Paleocene deep-water sediments and radiolarian faunas: Implications for evolution of Yarlung-Zangbo foreland basin, southern Tibet. *Sci. China Ser. D. Earth Sci.* **46**, 84-96 (2003).
- Jadoul, F., Berra, F. & Garzanti, E. The Tethys Himalayan passive margin from Late Triassic to Early Cretaceous (South Tibet). *J. Asian Earth Sci.* **16**, 173-194 (1998).
- Hu, X. *et al.* The timing of India-Asia collision onset Facts, theories, controversies. *Earth-Sci. Rev.* **160**, 264-299 (2016).
- Ding, L. *et al.* Processes of initial collision and suturing between India and Asia. *Sci. China Earth Sci.*, 635-651 (2017).
- Searle, M. P. *et al.* The closing of the Tethys and the tectonics of the Himalaya. *Geol. Soc. Am. Bull.* **98**, 678-701 (1987).
- van Hinsbergen, D. J. J., Steinberger, B., Doubrovine, P. V. & Gassmoller, R. Acceleration and deceleration of India-Asia convergence since the Cretaceous: Roles of mantle plumes and continental collision. *J. Geophys. Res.* **116**, B06101 (2011).
- Yang, T. *et al.* New insights into the India-Asia collision process from Cretaceous paleomagnetic and geochronologic results in the Lhasa terrane. *Gondwana Res.* **28**, 625-641 (2015).
- van Hinsbergen, D. J. J. *et al.* Reconstructing Greater India: Paleogeographic, kinematic, and geodynamic perspectives. *Tectonophysics* **760**, 69-94 (2019).
- Yuan, J. *et al.* Rapid drift of the Tethyan Himalaya terrane before two-stage India-Asia collision. *Natl. Sci. Rev.* **8**, nwaa173 (2021).
- Huang, W. et al. Remagnetization of the Paleogene Tibetan Himalayan carbonate rocks in the Gamba area: Implications for reconstructing the lower plate in the India-Asia collision. J. Geophys. Res. Solid Earth 122, 808–825 (2017).
- Rowley, D. B. Comparing paleomagnetic study means with apparent wander paths: A case study and paleomagnetic test of the Greater India versus Greater Indian Basin hypotheses. *Tectonics* **38**, 722-740 (2019).
- 64 Garzanti, E. & Hu, X. Latest Cretaceous Himalayan tectonics: Obduction, collision or

- Deccan-related uplift? Gondwana Res. 28, 165-178 (2015).
- Aitchison, J. C. *et al.* Remnants of a Cretaceous intra-oceanic subduction system within the Yarlung-Zangbo suture (southern Tibet). *Earth Planet. Sci. Lett.* **183**, 231-244 (2000).
- Jagoutz, O., Royden, L., Holt, A. F. & Becker, T. W. Anomalously fast convergence of India and Eurasia caused by double subduction. *Nat. Geosci.* **8**, 475-479 (2015).
- 67 Martin, C. R. *et al.* Paleocene latitude of the Kohistan-Ladakh arc indicates multistage India-Eurasia collision. *Proc. Natl. Acad. Sci. U. S. A.*, 29487-29494 (2020).
- Van der Voo, R., Spakman, W. & Bijwaard, H. Tethyan subducted slabs under India. *Earth Planet. Sci. Lett.* **171**, 7-20 (1999).
- DeCelles, P. G., Kapp, P., Gehrels, G. E. & Ding, L. Paleocene-Eocene foreland basin evolution in the Himalaya of southern Tibet and Nepal: implications for the age of initial India-Asia collision. *Tectonics* **33**, 824-849 (2014).
- Hu, X., Garzanti, E., Moore, T. & Raffi, I. Direct stratigraphic dating of India-Asia collision onset at the Selandian (middle Paleocene, 59 ± 1 Ma). *Geology* **43**, 859-862 (2015).
- Ding, L., Kapp, P. & Wan, X. Paleocene Eocene record of ophiolite obduction and initial India-Asia collision, south-central Tibet. *Tectonics* **24**, TC3001 (2005).
- Meng, J., Gilder, S. A., Li, Y., Wang, C. & Liu, T. Expanse of Greater India in the late Cretaceous. *Earth Planet. Sci. Lett.* **542**, 116330 (2020).
- Ding, L. *et al.* The India-Asia collision in north Pakistan: Insight from the U-Pb detrital zircon provenance of Cenozoic foreland basin. *Earth Planet. Sci. Lett.* **455**, 49-61 (2016).
- Qasim, M. *et al.* Tectonic implications of detrital zircon ages from Lesser Himalayan Mesozoic-Cenozoic strata, Pakistan. *Geochem., Geophys., Geosyst.* **19**, 1636-1659 (2018).
- Baral, U. *et al.* Detrital zircon U-Pb geochronology of a Cenozoic foreland basin in Northeast India: Implications for zircon provenance during the collision of the Indian and Asian plates. *Terra Nova* **31**, 18-27 (2019).
- Klootwijk, C. T., Conaghan, P. J. & Powell, C. M. The Himalayan Arc: large-scale continental subduction, oroclinal bending and back-arc spreading. *Earth Planet. Sci. Lett.* **75**, 167-183 (1985).
- Rowley, D. B. Age of initiation of collision between India and Asia: A review of stratigraphic data. *Earth Planet. Sci. Lett.* **145**, 1-13 (1996).
- Garzione, C. N., Quade, J., DeCelles, P. G. & English, N. B. Predicting paleoelevation of Tibet and the Himalaya from $\delta^{18}O$ vs. altitude gradients in meteoric water across the Nepal Himalaya. *Earth Planet. Sci. Lett.* **183**, 215-229 (2000).
- Rowley, D. B., Pierrehumbert, R. T. & Currie, B. S. A new approach to stable isotope-based paleoaltimetry: implications for paleoaltimetry and paleohypsometry of the High Himalaya since the Late Miocene. *Earth Planet. Sci. Lett.* **188**, 253-268 (2001).
- Quade, J., Breecker, D., Daeron, M. & Eiler, J. The paleoaltimetry of Tibet: an isotopic perspective. *Am. J. Sci.* **311**, 77-115 (2011).
- Li, L. & Garzione, C. N. Spatial distribution and controlling factors of stable isotopes in meteoric waters on the Tibetan Plateau: Implications for paleoelevation reconstruction. *Earth Planet. Sci. Lett.* **460**, 302-314 (2017).
- Quade, J. *et al.* Resetting Southern Tibet: The serious challenge of obtaining primary records of Paleoaltimetry. *Glob. Planet. Change* **191**, 103194 (2020).
- Wei, Y. et al. Low palaeoelevation of the northern Lhasa terrane during late Eocene: Fossil

- foraminifera and stable isotope evidence from the Gerze Basin. Sci. Rep. 6, 27508 (2016).
- Huang, W. *et al.* Hydrothermal events in the Linzizong Group: Implications for Paleogene exhumation and paleoaltimetry of the southern Tibetan Plateau. *Earth Planet. Sci. Lett.* **583**, 117390 (2022).
- Currie, B. S. *et al.* Multiproxy paleoaltimetry of the Late Oligocene-Pliocene Oiyug Basin, southern Tibet. *Am. J. Sci.* **316**, 401-436 (2016).
- Ingalls, M., Rowley, D. B., Currie, B. S. & Colman, A. S. Reconsidering the uplift history and peneplanation of the northern Lhasa terrane, Tibet. *Am. J. Sci.* **320**, 479-532 (2020).
- Xiong, Z. *et al.* The rise and demise of the Paleogene Central Tibetan Valley. *Sci. Adv.* **8**, eabj0944 (2022).
- Wang, Z., Schauble, E. A. & Eiler, J. M. Equilibrium thermodynamics of multiply substituted isotopologues of molecular gases. *Geochim. Cosmochim. Acta.* **69**, 4779-4797 (2004).
- 89 Eiler, J. M. "Clumped-isotope" geochemistry—The study of naturally-occurring, multiply substituted isotopologues. *Earth Planet. Sci. Lett.* **262**, 309-327 (2007).
- 90 Spicer, R. A. *et al.* Constant elevation of southern Tibet over the past 15 million years. *Nature* **421**, 622-624 (2003).
- 91 Su, T. *et al.* A Middle Eocene lowland humid subtropical "Shangri-La" ecosystem in central Tibet. *Proc. Natl. Acad. Sci. U. S. A.*, 32989-32995 (2020).
- 92 Botsyun, S. & Ehlers, T. A. How can climate models be used in paleoelevation reconstructions? Front. Earth Sci. 9, 624542 (2021).
- 93 Botsyun, S., Sepulchre, P., Risi, C. & Donnadieu, Y. Impacts of Tibetan Plateau uplift on atmospheric dynamics and associated precipitation d¹⁸O. *Climate of the Past Discussions, European Geosciences Union (EGU)* 12, 1401-1420 (2016).
- Shen, H. & Poulsen, C. J. Precipitation d¹⁸O on the Himalaya-Tibet orogeny and its relationship to surface elevation. *Clim. Past* **15**, 169-187 (2019).
- Botsyun, S. *et al.* Revised paleoaltimetry data show low Tibetan Plateau elevation during the Eocene. *Science* **363**, eaaq1436 (2019).
- Valdes, P. J. *et al.* Comment on "Revised paleoaltimetry data show low Tibetan Plateau elevation during the Eocene". *Science*, 10.1126/science.aax8474 (2019).
- 97 Botsyun, S. *et al.* Response to Comment on "Revised paleoaltimetry data show low Tibetan Plateau elevation during the Eocene". *Science*, doi:10.1126/science.aax8990 (2019).
- 98 Xu, Q. et al. Paleogene high elevations in the Qiangtang Terrane, central Tibetan Plateau. Earth Planet. Sci. Lett. **362**, 31-42 (2013).
- Ingalls, M. *et al.* Paleocene to Pliocene low-latitude, high-elevation basins of southern Tibet: Implications for tectonic models of India-Asia collision, Cenozoic climate, and geochemical weathering. *Geol. Soc. Am. Bull.* **130**, 307-330 (2018).
- Spicer, R. A. *et al.* Why 'the uplift of the Tibetan Plateau' is a myth? *Natl. Sci. Rev.* **8**, nwaa091 (2020).
- DeCelles, P. G., Kapp, P., Quade, J. & Gehrels, G. E. Oligocene-Miocene Kailas Basin, southwestern Tibet: Record of postcollisional upper-plate extension in the Indus-Yarlung suture zone. *Geol. Soc. Am. Bull.* **123**, 1337-1362 (2011).
- Ding, L., Kapp, P., Zhong, D. & Deng, W. Cenozoic volcanism in Tibet: evidence for a transition from oceanic to continental subduction. *J. Petrol.* **44**, 1833-1865 (2003).
- Leech, M. L., Singh, S., Jain, A. K., Klemperer, S. L. & Manickavasagam, R. M. The onset of

- India-Asia continental collision: Early, steep subduction required by the timing of UHP metamorphism in the western Himalaya. *Earth Planet. Sci. Lett.* **234**, 83-97 (2005).
- Ding, L. *et al.* Quantifying the rise of the Himalaya orogen and implications for the South Asian monsoon. *Geology* **45**, 215-218 (2017).
- Orme, D. A., Carrapa, B. & Kapp, P. Sedimentology, provenance and geochronology of the upper Cretaceous-lower Eocene western Xigaze forearc basin, southern Tibet. *Basin Res.* **27**, 387-411 (2015).
- Najman, Y. *et al.* Timing of India-Asia collision: Geological, biostratigraphic, and palaeomagnetic constraints. *J. Geophys. Res.* **115**, B12416 (2010).
- Zhang, Q., Willems, H., Ding, L., Grafe, K.-U. & Appel, E. Initial India-Asia continental collision and foreland basin evolution in the Tethyan Himalaya of Tibet: Evidence from stratigraphy and paleontology. J. Geol. 120, 175-189 (2012).
- Currie, B. S., Rowley, D. B. & Tabor, N. J. Middle Miocene paleoaltimetry of southern Tibet: Implications for the role of mantle thickening and delamination in the Himalayan orogen. *Geology* **33**, 181-184 (2005).
- Khan, M. A. *et al.* Miocene to Pleistocene floras and climate of the Eastern Himalayan Siwaliks, and new palaeoelevation estimates for the Namling-Oiyug Basin, Tibet. *Glob. Planet. Change* **113**, 1-10 (2014).
- Bai, Y., Chen, C., Xu, Q. & Fang, X. Paleoaltimetry potentiality of branched GDGTs from southern Tibet. *Geochem., Geophys., Geosyst.* **19**, 551-564 (2018).
- 111 Chung, S.-L. *et al.* Tibetan tectonic evolution inferred from spatial and temporal variations in post-collisional magmatism. *Earth-Sci. Rev.* **68**, 173-196 (2005).
- Mo, X. *et al.* Mantle contributions to crustal thickening during continental collision: Evidence from Cenozoic igneous rocks in southern Tibet. *Lithos* **96**, 225-242 (2007).
- Patriat, P. & Achache, J. India-Eurasia collision chronology has implications for crustal shortening and driving mechanism of plates. *Nature* **311**, 615-620 (1984).
- Gibbons, A. D., Zahirovic, S., Müller, R. D., Whittaker, J. M. & Yatheesh, V. A tectonic model for reconciling evidence for the collisions between India, Eurasia and intra-oceanic arcs of the central-eastern Tethys. *Gondwana Res.* 28, 451-492 (2015).
- Laskowski, A. K., Kapp, P., Ding, L., Campbell, C. & Liu, X. H. Tectonic evolution of the Yarlung suture zone, Lopu Range region, southern Tibet. *Tectonics* **36**, 108-136 (2017).
- Ding, L., Kapp, P., Yue, Y. & Lai, Q. Postcollisional calc-alkaline lavas and xenoliths from the southern Qiangtang terrane, central Tibet. *Earth Planet. Sci. Lett.* **254**, 28-38 (2007).
- Guo, Z. & Wilson, M. Late Oligocene-early Miocene transformation of postcollisional magmatism in Tibet. *Geology* **47**, 776-780 (2019).
- Li, Y., Wang, C., Zhao, X., Yin, A. & Ma, C. Cenozoic thrust system, basin evolution, and uplift of the Tanggula Range in the Tuotuohe region, central Tibet. *Gondwana Res.* **22**, 482-492 (2012).
- Law, R. & Allen, M. B. Diachronous Tibetan Plateau landscape evolution derived from lava field geomorphology. *Geology* **48**, 263-267 (2020).
- 120 Kapp, P. *et al.* Tectonic evolution of the early Mesozoic blueschist-bearing Qiangtang metamorphic belt, central Tibet. *Tectonics* **22**, 1043 (2003).
- Pullen, A., Kapp, P., Gehrels, G. E., Ding, L. & Zhang, Q. Metamorphic rocks in central Tibet: Lateral variations and implications for crustal structure. *Geol. Soc. Am. Bull.* **123**, 585-600

(2011).

- 122 Clark, M. K. *et al.* Use of a regional, relict landscape to measure vertical deformation of the eastern Tibetan Plateau. *J. Geophys. Res.* **111**, F03002 (2006).
- Horton, B. K., Yin, A., Spurlin, M. S., Zhou, J. & Wang, J. Paleocene-Eocene syncontractional sedimentation in narrow, lacustrine-dominated basins of east-central Tibet. *Geol. Soc. Am. Bull.* **114**, 771-786 (2002).
- Spurlin, M. S., Yin, A., Horton, B. K., Zhou, J. & Wang, J. Structural evolution of the Yushu-Nangqian region and its relationship to syncollisional igneous activity, east-central Tibet. *Geol. Soc. Am. Bull.* **117**, 1293-1317 (2005).
- Li, L. *et al.* Carbonate stable and clumped isotopic evidence for late Eocene moderate to high elevation of the east-central Tibetan Plateau and its geodynamic implications. *Geol. Soc. Am. Bull.* **131**, 831-844 (2018).
- 126 Xiong, Z. *et al.* The early Eocene rise of the Gonjo Basin, SE Tibet: From low desert to high forest. *Earth Planet. Sci. Lett.* **543**, 116312 (2020).
- Su, T. *et al.* Uplift, climate and biotic changes at the Eocene-Oligocene transition in south-eastern Tibet. *Natl. Sci. Rev.* **6**, 495-504 (2019).
- Liu-Zeng, J. *et al.* Multiple episodes of fast exhumation since Cretaceous in southeast Tibet, revealed by low-temperature thermochronology. *Earth Planet. Sci. Lett.* **490**, 62-76 (2018).
- Jackson Jr., W. T., Robinson, D. M., Weislogel, A. L., Jian, X. & McKay, M. P. Cenozoic development of the nonmarine Mula basin in the Southern Yidun terrane: Deposition and deformation in the eastern Tibetan Plateau associated with the India-Asia collision. *Tectonics* **37**, 2446-2465 (2018).
- Jackson Jr., W. T., Robinson, D. M., Weislogel, A. L. & Jian, X. Cenozoic reactivation along the Late Triassic Ganzi-Litang suture, eastern Tibetan Plateau. *Geosci. Front.* **11**, 1069-1080 (2020).
- Hoke, G. D., Liu-Zeng, J., Hren, M. T., Wissink, G. K. & Garzione, C. N. Stable isotopes reveal high southeast Tibetan Plateau margin since the Paleogene. *Earth Planet. Sci. Lett.* **394**, 270-278 (2014).
- Nie, J. *et al.* Rapid incision of the Mekong River in the middle Miocene linked to monsoonal precipitation. *Nat. Geosci.*, 944-948 (2018).
- Xu, Q., Ding, L., Hetzel, R., Yue, Y. & Rades, E. F. Low elevation of the northern Lhasa terrane in the Eocene: Implications for relief development in south Tibet. *Terra Nova* **27**, 458-466 (2015).
- Wu, F., Miao, D., Chang, M.-m., Shi, G. & Wang, N. Fossil climbing perch and associated plant megafossils indicate a warm and wet central Tibet during the late Oligocene. *Sci. Rep.* **7**, 878 (2017).
- Fang, X. et al. Revised chronology of central Tibet uplift (Lunpola Basin). Sci. Adv. 6, eaba7298 (2020).
- Polissar, P. J., Freeman, K. H., Rowley, D. B., McInerney, F. A. & Currie, B. S. Paleoaltimetry of the Tibetan Plateau from D/H ratios of lipid biomarkers. *Earth Planet. Sci. Lett.* **287**, 64-76 (2009).
- DeCelles, P. G. *et al.* High and dry in central Tibet during the Late Oligocene. *Earth Planet. Sci. Lett.* **253**, 389-401 (2007).
- 138 Sun, J. et al. Palynological evidence for the latest Oligocene-early Miocene paleoelevation

- estimate in the Lunpola Basin, central Tibet. *Palaeogeogr. Palaeoclimatol. Palaeoecol.* **399**, 21-30 (2014).
- Farnsworth, A. *et al.* Paleoclimate model-derived thermal lapse rates: Towards increasing precision in paleoaltimetry studies. *Earth Planet. Sci. Lett.* **564**, 116903 (2021).
- Li, Z.-H., Liu, M. & Gerya, T. Lithosphere delamination in continental collisional orogens: A systematic numerical study. *J. Geophys. Res. Solid Earth* **121**, 5186-5211 (2016).
- DeCelles, P. G., Robinson, D. M. & Zandt, G. Implications of shortening in the Himalayan fold-thrust belt for uplift of the Tibetan Plateau. *Tectonics* **21**, 1062 (2002).
- Kelly, S., Butler, J. P. & Beaumont, C. Continental collision with a sandwiched accreted terrane: Insights into Himalayan-Tibetan lithospheric mantle tectonics? *Earth Planet. Sci. Lett.* **455**, 176-195 (2016).
- Husson, L. et al. Dynamic ups and downs of the Himalaya. Geology 42, 839-842 (2014).
- Leary, R. *et al.* Along-strike diachroneity in the deposition of the Kailas Formation in central southern Tibet: Implications for Indian slab dynamics. *Geosphere* **12**, 1198-1223 (2016).
- Kohn, M. J. Himalayan metamorphism and its tectonic implications. *Annu. Rev. Earth Planet. Sci.* **42**, 381-419 (2014).
- Wang, J.-M. *et al.* First evidence of eclogites overprinted by ultrahigh temperature metamorphism in Everest East, Himalaya: Implications for collisional tectonics on early Earth. *Earth Planet. Sci. Lett.* **558**, 116760 (2021).
- Searle, M. P., Cottle, J. M., Streule, M. J. & Waters, D. J. Crustal melt granites and migmatites along the Himalaya: melt sources, segregation, transport and granite emplacement mechanisms. *Earth and Environmental Science Transactions of the Royal Society of Edinbrugh* **100**, 219-233 (2010).
- Lin, C. *et al.* Himalayan Miocene adakitic rocks, a case study of the Mayum pluton: Insights into geodynamic processes within the subducted Indian continental lithosphere and Himalayan mid-Miocene tectonic regime transition. *Geol. Soc. Am. Bull.* **133**, 591-611 (2021).
- DeCelles, P. G. *et al.* Oligocene-Miocene Great Lakes in the India-Asia Collision Zone. *Basin Res.* **30**, 228-247 (2016).
- Xu, Q. *et al.* Stable isotopes reveal southward growth of the Himalayan-Tibetan Plateau since the Paleocene. *Gondwana Res.* **54**, 50-61 (2018).
- 151 Gébelin, A. et al. The Miocene elevation of Mount Everest. Geology 41, 799-802 (2013).
- Gébelin, A. *et al.* Infiltration of meteoric water in the South Tibetan Detachment (Mount Everest, Himalaya): When and why? *Tectonics* **36**, 690-713 (2017).
- Garzione, C. N., Dettman, D. L., Quade, J., DeCelles, P. G. & Butler, R. F. High times on the Tibetan plateau: Paleoelevation of the Thakkhola graben, Nepal. *Geology* **28**, 339-342 (2000).
- Saylor, J. E. *et al.* The Late Miocene through present paleoelevation history of southwestern Tibet. *Am. J. Sci.* **309**, 1-42 (2009).
- Murphy, M. A., Saylor, J. E. & Ding, L. Late Miocene topographic inversion in southwest Tibet based on integrated paleoelevation reconstructions and structural history. *Earth Planet. Sci. Lett.* **282**, 1-9 (2009).
- Huntington, K. W., Saylor, J., Quade, J. & Hudson, A. M. High late Miocene-Pliocene elevation of the Zhada Basin, southwestern Tibetan Plateau, from carbonate clumped isotope thermometry. *Geol. Soc. Am. Bull.* **127**, 181-199 (2015).
- 157 Clift, P. D. et al. Correlation of Himalayan exhumation rates and Asian monsoon intensity. Nat.

- Geosci. 1, 875-880 (2008).
- 158 Clift, P. D. & Webb, A. A. G. in *Himalayan Tectonics: A Modern Synthesis* (eds P. J. Treloar & M. P. Searle) 631-652 (Geological Society of London Special Publications 483, 2019).
- Cyr, A. J., Currie, B. S. & Rowley, D. B. Geochemical evaluation of Fenghuoshan Group lacustrine carbonates, north-central Tibet: Implications for the paleoaltimetry of the Eocene Tibetan Plateau. *J. Geol.* **113**, 517-533 (2005).
- Miao, Y. *et al.* A Late-Eocene palynological record from the Hoh Xil Basin, northern Tibetan Plateau, and its implications for stratigraphic age, paleoclimate and paleoelevation. *Gondwana Res.* **31**, 241-252 (2016).
- Staisch, L. M., Niemi, N. A., Clark, M. K. & Chang, H. Eocene to late Oligocene history of crustal shortening within the Hoh Xil Basin and implications for the uplift history of the northern Tibetan Plateau. *Tectonics* **35**, 862-895 (2016).
- Sun, B. *et al.* Early Miocene elevation in northern Tibet estimated by palaeobotanical evidence. *Sci. Rep.* **5**, 10379 (2015).
- Wu, Z., Barosh, P. J., Hu, D., Zhao, X. & Ye, P. Vast early Miocene lakes of the central Tibetan Plateau. *Geol. Soc. Am. Bull.* **120**, 1326-1337 (2008).
- Yin, A., Dang, Y.-Q., Zhang, M., Chen, X.-H. & McRivette, M. W. Cenozoic tectonic evolution of the Qaidam basin and its surrounding regions (Part 3): Structural geology, sedimentation, and regional tectonic reconstruction. *Geol. Soc. Am. Bull.* **120**, 847-876 (2008).
- McRivette, M. W., Yin, A., Chen, X. & Gehrels, G. E. Cenozoic basin evolution of the central Tibetan plateau as constrained by U-Pb detrital zircon geochronology, sandstone petrology, and fission-track thermochronology. *Tectonophysics* **751**, 150-179 (2019).
- Yuan, D.-Y. *et al.* The growth of northeastern Tibet and its relevance to large-scale continental geodynamics: A review of recent studies. *Tectonics* **32**, 1358-1370 (2013).
- Wu, C. et al. Late Mesozoic-Cenozoic cooling history of the northeastern Tibetan Plateau and its foreland derived from low-temperature thermochronology. *Geol. Soc. Am. Bull.*, 2393–2417 (2021).
- Styron, R., Taylor, M. & Sundell, K. Accelerated extension of Tibet linked to the northward underthrusting of Indian crust. *Nat. Geosci.* **8**, 131-134 (2015).
- Taylor, M., Forte, A., Laskowski, A. & Ding, L. Active uplift of southern Tibet revealed. *GSA Today* **31**, 4-10 (2021).
- Owens, T. J. & Zandt, G. Implications of crustal property variations for models of Tibetan plateau evolution. *Nature* **387**, 37-43 (1997).
- Tilmann, F., Ni, J. & Team, I. I. S. Seismic imaging of the downwelling Indian lithosphere beneath central Tibet. *Science* **300**, 1424-1427 (2003).
- Nábělek, J. L. *et al.* Underplating in the Himalaya-Tibet collision zone revealed by the Hi-CLIMB experiment. *Science* **325**, 1371-1374 (2009).
- Zhao, J. et al. The boundary between the Indian and Asian tectonic plates below Tibet. PNAS25, 11229-11233 (2010).
- Li, C., van der Hilst, R. D., Meltzer, A. S. & Engdahl, E. R. Subduction of the Indian lithosphere beneath the Tibetan Plateau and Burma. *Earth Planet. Sci. Lett.* **274**, 157-168 (2008).
- 275 Zhao, W. *et al.* Tibetan plate overriding the Asian plate in central and northern Tibet. *Nat. Geosci.* **4**, 870-873 (2011).
- 176 Liang, X. et al. 3D imaging of subducting and fragmenting Indian continental lithosphere

- beneath southern and central Tibet using body-wave fine-frequency tomography. *Earth Planet. Sci. Lett.* **443**, 162-175 (2016).
- Liang, X. et al. A complex Tibetan upper mantle: A fragmented Indian slab and no south-verging subduction of Eurasian lithosphere. Earth Planet. Sci. Lett. 333-334, 101-111 (2012).
- 178 Chen, Y., Li, W., Yuan, X., Badal, J. & Teng, J. Tearing of the Indian lithospheric slab beneath southern Tibet revealed by SKS-wave splitting measurements. *Earth Planet. Sci. Lett.* **413**, 13-24 (2015).
- Yin, A. Mode of Cenozoic east-west extension in Tibet suggesting a common origin of rifts in Asia during the Indo-Asian collision. *J. Geophys. Res.* **105**, 21745-21759 (2000).
- 180 Kind, R. *et al.* Seismic images of crust and upper mantle beneath Tibet: Evidence for Eurasian plate subduction. *Science* **298**, 1219-1221 (2002).
- Kumar, P., Yuan, X., Kind, R. & Ni, J. Imaging the colliding Indian and Asian lithospheric plates beneath Tibet. *J. Geophys. Res.* **111**, B06308 (2006).
- Feng, M. *et al.* Structure of the crust and mantle down to 700 km depth beneath the East Qaidam basin and Qilian Shan from P and S receiver functions. *Geophys. J. Int.* **199**, 1416-1429 (2014).
- Sippl, C. *et al.* Geometry of the Pamir-Hindu Kush intermediate-depth earthquake zone from local seismic data. *J. Geophys. Res.* **118**, 1438-1457 (2013).
- Kufner, S.-K. *et al.* Deep India meets deep Asia: Lithospheric indentation, delamination and break-off under Pamir and Hindu Kush (Central Asia). *Earth Planet. Sci. Lett.* **435**, 171-184 (2016).
- Kufner, S.-K. *et al.* The Hindu Kush slab break-off as revealed by deep structure and crustal deformation. *Nat. Commun.* **12**, 1685 (2021).
- Schneider, F. M. *et al.* Seismic imaging of subducting continental lower crust beneath the Pamir. *Earth Planet. Sci. Lett.* **375**, 101-112 (2013).
- 187 Replumaz, A., Negredo, A. M., Villasenor, A. & Guillot, S. Indian continental subduction and slab break-off during Tertiary collision. *Terra Nova* **22**, 290-296 (2010).
- Wittlinger, G. *et al.* Teleseismic imaging of subducting lithosphere and Moho offsets beneath western Tibet. *Earth Planet. Sci. Lett.* **221**, 117-130 (2004).
- Schulte-Pelkum, V. *et al.* Imaging the Indian subcontinent beneath the Himalaya. *Nature* **435**, 1222-1225 (2005).
- Hetényi, G. *et al.* Density distribution of the India plate beneath the Tibetan plateau: Geophysical and petrological constraints on the kinetics of lower-crustal eclogitization. *Earth Planet. Sci. Lett.* **264**, 226-244 (2007).
- 191 Shi, D., Klemperer, S. L., Shi, J., Wu, Z. & Zhao, W. Localized foundering of Indian lower crust in the India-Tibet collision zone. *PNAS* **117**, 24742-24747 (2020).
- McNamara, D. E., Walter, W. R., Owens, T. J. & Ammon, C. J. Upper mantle velocity structure beneath the Tibetan Plateau from Pn travel time tomography. *J. Geophys. Res.* **102**, 493-505 (1997).
- 2hao, W. *et al.* Crustal structure of central Tibet as derived from project INDEPTH wide-angle seismic data. *Geophys. J. Int.* **145**, 486-498 (2001).
- Barron, J. & Priestley, K. Observations of frequency-dependent Sn propagation in Northern Tibet. *Geophys. J. Int.* **179**, 475-488 (2009).

- Jimenez-Munt, I., Fernandez, M., Verges, J. & Platt, J. P. Lithopshere structure underneath the Tibetan Plateau inferred from elevation, gravity and geoid anomalies. *Earth Planet. Sci. Lett.* **267**, 276-289 (2008).
- 196 Chen, M. *et al.* Lithospheric foundering and underthrusting imaged beneath Tibet. *Nat. Commun.* **8**, 15659 (2017).
- Liang, S. M. *et al.* Three-dimensional velocity field of present-day crustal motion of the Tibetan Plateau derived from GPS measurements. *J. Geophys. Res. Solid Earth* **118**, 5722-5732 (2013).
- Nelson, K. D. *et al.* Partially molten middle crust beneath southern Tibet: Synthesis of Project INDEPTH results. *Nature* **274**, 1684-1688 (1996).
- 199 Gao, R. *et al.* Crustal-scale duplexing beneath the Yarlung Zangbo suture in the western Himalaya. *Nat. Geosci.* **9**, 555-560 (2016).
- 200 Makovsky, Y., Klemperer, S. L., Ratschbacher, L. & Alsdorf, D. Midcrustal reflector on INDEPTH wide-angle profiles: An ophiolitic slab beneath the India-Asia suture in southern Tibet? *Tectonics* **18**, 793-808 (1999).
- Sternai, P. *et al.* On the influence of the asthenospheric flow on the tectonics and topography at a collision-subduction transition zones: Comparison with the eastern Tibetan margin. *J. Geodyn.* **100**, 184-197 (2016).
- Jolivet, L. *et al.* Mantle flow and deforming continents: From India-Asia convergence to Pacific subduction. *Tectonics* **37**, 2887-2914 (2018).
- Faccenna, C., Becker, T. W., Conrad, C. P. & Husson, L. Mountain building and mantle dynamics. *Tectonics* **32**, 80-93 (2013).
- Powell, C. M. & Conaghan, P. J. Plate tectonics and the Himalayas. *Earth Planet. Sci. Lett.* **20**, 1-12 (1973).
- Zhao, W.-L. & Morgan, W. J. Injection of Indian crust into Tibetan lower crust: A two-dimensional finite element model study. *Tectonics* **6**, 489-504 (1987).
- Ai, K. K. *et al.* The uppermost Oligocene Kailas flora from southern Tibetan Plateau and its implications for the uplift history of the southern Lhasa terrane. *Palaeogeogr. Palaeoclimatol. Palaeoecol.* **515**, 143-151 (2019).
- 207 Chen, C. *et al.* Lower-altitude of the Himalayas before the mid-Pliocene as constrained by hydrological and thermal conditions. *Earth Planet. Sci. Lett.* **545**, 116422 (2020).
- Xu, Q., Li, S. & Bai, Y. Modern-like elevation and climate in Tibet since the mid-Miocene (ca. 15 Ma). *Geol. Soc. Am. Bull.*, doi.org/10.1130/B36198.36191 (2022).
- Jia, G., Bai, Y., Ma, Y., Sun, J. & Peng, P. Paleoelevation of Tibetan Lunpola basin in the Oligocene-Miocene transition estimated from leaf wax lipid dual isotopes. *Glob. Planet. Change* **126**, 14-22 (2015).
- Wu, J. *et al.* Paleoelevations in the Jianchuan Basin of the southeastern Tibetan Plateau based on stable isotope and pollen grain analyses. *Palaeogeogr. Palaeoclimatol. Palaeoecol.* **510**, 93-108 (2018).
- Li, S., Currie, B. S., Rowley, D. B. & Ingalls, M. Cenozoic paleoaltimetry of the SE margin of the Tibetan Plateau: Constraints on the tectonic evolution of the region. *Earth Planet. Sci. Lett.* **432**, 415-424 (2015).
- Dal Zilio, L., Het é nyi, G., Hubbard, J. & Bollinger, L. Building the Himalaya from tectonic to earthquake scales. *Nature Reviews Earth and Environment*, 251-268 (2021).

- 213 Kar, N. *et al.* Rapid regional surface uplift of the northern Altiplano plateau revealed by multiproxy paleoclimate reconstruction. *Earth Planet. Sci. Lett.* **447**, 33-47 (2016).
- Yang, J., Spicer, R. A., Spicer, T. E. V. & Li, C.-S. 'CLAMP Online': a new web-based palaeoclimate tool and its application to the terrestrial Paleogene and Neogene of North America. *Palaeobio. Palaeoenv.* **91**, 163-183 (2011).
- Forest, C. E., Wolfe, J. A., Molnar, P. & Emanuel, K. A. Paleoaltimetry incorporating atmospheric physics and botanical estimates of paleoclimate. *Geol. Soc. Am. Bull.* **111**, 497-511 (1999).
- Hopmans, E. C. *et al.* A novel proxy for terrestrial organic matter in sediments based on branched and isoprenoid tetraether lipids. *Earth Planet. Sci. Lett.* **224**, 107-116 (2004).
- Schouten, S., Hopmans, E. C. & Sinninghe Damst é, J. S. The organic geochemistry of glycerol dialkyl glycerol tetraether lipds: A review. *Org. Geochem.* **54**, 19-61 (2013).
- 218 Ghosh, P., Garzione, C. N. & Eiler, J. Rapid Uplift of the Altiplano Revealed Through ¹³C-¹⁸O Bonds in Paleosol Carbonates. *Science* **311**, 511-515 (2006).
- Garzione, C. N., Molnar, P., Libarkin, J. C. & MacFadden, B. J. Rapid late Miocene rise of the Bolivian Altiplano: Evidence for removal of mantle lithosphere. *Earth Planet. Sci. Lett.* **241**, 543-556 (2006).
- 220 Utescher, T. *et al.* The Coexistence Approach —Theoretical background and practical considerations of using plant fossils for climate quantification. *Palaeogeogr. Palaeoclimatol. Palaeoecol.* **410**, 58-73 (2014).